Light-driven Rotary Molecular Motors for Out-of-Equilibrium Systems

Lubbe, Anouk S.; Stähler, Cosima L.G.; Feringa, Ben L.

Published in:
Out-of-Equilibrium (Supra)molecular Systems and Materials

DOI:
10.1002/9783527821990.ch12

Publication date:
2021

12

Light-driven Rotary Molecular Motors for Out-of-Equilibrium Systems

Anouk S. Lubbe, Cosima L.G. Stähler, and Ben L. Feringa

University of Groningen, Faculty of Science and Engineering, Nijenborgh 4, 9747 AG Groningen, The Netherlands

12.1 Introduction

Less than 150 years since De Lavoisier laid the foundations of modern chemistry, chemists have created a marvelous diversity of molecules and accumulated an unimaginable wealth of information on materials. NMR and MS techniques allow us to determine exact molecular compositions within minutes, scanning tunneling microscopy allows us to look at individual atoms [1], and advanced spectroscopic methods and X-ray crystallography can establish the exact 3D structure of complex proteins and their binding pockets [2], after which structure-based design can be used to prepare a drug tailor made to fit that pocket [3]. However, the days of chemistry as the science of the single molecule have long passed, as evident from the rise of, e.g. supramolecular chemistry. The boundaries between chemistry and physics or biology have all but disappeared, and chemistry is no longer restrained to the nanoscale. By joining forces with other disciplines, we are able to traverse length scales and understand the properties of matter anywhere between the pico- and the macroscale. Bottom-up design of molecules and the interaction between larger assemblies let us create new materials, tailor made for their envisioned application by translating molecular properties to real-life functions.

Responsive or "smart" materials can change their properties in response to an external trigger and by now are able to perform the most amazing tasks. Self-healing materials autonomously repair damage [4], soft actuators perform biomimetic tasks on the macroscale [5], and smart drug delivery systems can circumvent the devastating side effects associated with some treatments [6]. In the continuing quest to create more advanced materials, achieving mechanical actuation and other life-like motion at the macroscale is a major landmark, and some inspiring examples have been reported [7, 8]. However, many of these responsive systems are limited to reversible (switching) motion in which no net work is generated. If the ultimate goal is to create a smart material capable of performing real work at the nanoscale, chemists need to take inspiration from nature. In contrast to the vast majority of

Out-of-Equilibrium (Supra)molecular Systems and Materials, First Edition.
Edited by Nicolas Giuseppone and Andreas Walther.

newly created artificial chemical systems, life takes place away from equilibrium. A living body capable of performing work, such as moving around or reading this chapter, needs to be sustained by a continuous input of fuel, or it will soon reach equilibrium and die. Likewise, at the molecular scale, in order to perform work, a molecule or material needs to operate away from the thermodynamic equilibrium. Moreover, a dissipative system is required in which the energy is dispersed via irreversible processes [9]. This definition disqualifies systems such as switches, which may operate away from thermal equilibrium yet still reside in another local minimum, such as a metastable state [10]. Fortunately, while life has motor proteins to drive the motion of life [11], chemists have designed molecular machines to drive the smart materials and nanomachinery of the future [12–17].

The principle of microscopic reversibility states that "in a reversible reaction, the mechanism in one direction is exactly the reverse of the mechanism in the other direction" [18]. Therefore, at equilibrium only a Boltzmann distribution is expected, and no net work can be performed. Biological molecular motors are able to circumvent this and drive directed motion via adenosine triphosphate (ATP) hydrolysis [19]. In order to perform work, we too need to get away from thermal equilibrium by bypassing microscopic reversibility [20]. How to do that is easily revealed by the second line of the IUPAC definition of microscopic reversibility: "[Microscopic reversibility] does not apply to reactions that begin with a photochemical excitation" [18].

When considering the driving force for the responsive systems, smart materials, and nanomachinery of the future, light stands out in most, if not all, aspects. Light can be applied with high spatiotemporal control and can be easily varied in terms of intensity and wavelength. It leaves no waste products and can therefore be used to drive a closed system. Visible light in particular is abundantly present and an environmentally friendly energy source. For operating away from equilibrium, light offers the ultimate advantage: the ability to circumvent microscopic reversibility. A light-driven process passes through the excited state, yet can return thermally via the ground state. This "loophole" allows us to desymmetrize the energy landscape and therefore block backward reactions. The resulting irreversible directional movement across the energy landscape can be exploited to generate net work. A combination of photochemical and thermal isomerizations can therefore be used to construct a molecular machine, capable of continuous directional movement.

Light-driven rotary molecular motors are a highly versatile class of molecular machines that have been developed and intensively studied in our group over the past 20 years. Originally based on a class of helical overcrowded alkene-based molecular switches related to stilbenes [21], the introduction of two stereocenters adjacent to the central double bond imposes unidirectionality of rotation (Scheme 12.1). Although some functional chemically fueled unidirectional motors have been reported [22–25], light remains the preferred source of energy for applications in responsive materials.

In this chapter, we will discuss whether rotary molecular motors are able to operate away from thermal equilibrium, if this implies that they are capable to perform work, and whether this work on the molecular scale can be amplified across length scales. After a very brief discussion on the basic requirements for

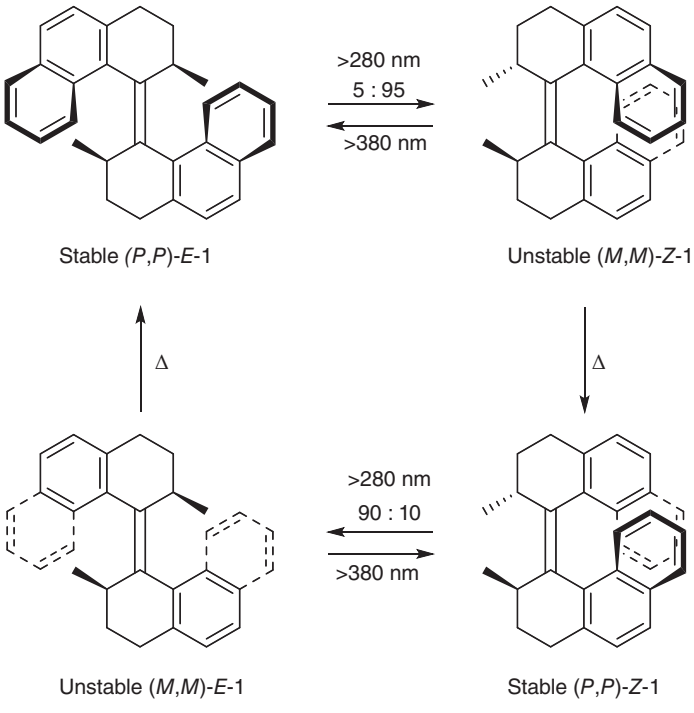

Scheme 12.1 Mechanism of the 360° unidirectional rotation of first-generation molecular motor **1**.

a molecular system to perform work, we will discuss light-driven rotary motors. This discussion will include a detailed explanation of the rotary cycle, the various core designs thus far developed, and several strategies toward tuning the properties of rotary molecular motors, including speed of rotation, wavelength of excitation, etc. Subsequently we will describe the out-of-equilibrium properties of molecular motors and how these may be used to generate work. In the second half of this chapter, we will analyze examples from literature demonstrating the ability of molecular motors to perform work, starting with examples in which a net output is generated by single molecules, followed by larger (supramolecular) systems. We characterize the different strategies toward amplifying motor function in order to generate a response at larger length scales, with the ultimate goal of developing responsive materials that perform work at the macroscale. Finally, we conclude with a short review of the state of the art and an outlook to the future potential of rotary molecular motors operating out of equilibrium.

12.2 Design and Synthesis of Light-driven Rotary Motors

Scheme 12.1 depicts the rotation cycle of the first reported molecular motor **1** [26]. This symmetrical molecule, also referred to as a first-generation motor, features an

overcrowded and therefore highly twisted central double bond. Upon irradiation of the stable *E* isomer with UV light, isomerization around this double bond occurs, and a photochemical equilibrium (called photostationary state [PSS]) between the *Z* and *E* forms is established. As the methyl groups on the stereogenic centers change from a pseudoaxial to a pseudoequatorial orientation, this newly formed unstable *Z* isomer experiences additional strain around the central double bond. Such a higher energy isomer typically exhibits a redshifted absorption maximum, and as a result the equilibrium often lies far to the side of the unstable *Z* isomer. The additional strain caused by the equatorial position of the methyl groups in the unstable *Z* isomer can be relieved by a thermal helix inversion (THI) in which the halves of the motor slide past each other. This process results in formation of the stable *Z* isomer, in which the methyl groups are once again in a pseudoaxial orientation. The THI is irreversible under the reaction conditions and thus ensures unidirectionality. A repetition of the irradiation and subsequent thermal step completes the 360° unidirectional rotation. The speed of this process is highly variable and depends on multiple factors. The time it takes to reach PSS depends on light intensity, concentration, and quantum yield. For the thermal process, the half-life of the unstable *E* isomer of molecular motor **1** is estimated to be around 18 days, based on a very similar molecular motor [27]. The half-life of the unstable *Z* isomer is much shorter, estimated to be around 30 minutes. Characterization of the rotary cycle is relatively straightforward – a combination of NMR, UV, and CD spectroscopy is usually sufficient to prove unidirectionality and determine key values such as the half-life of the unstable states (i.e. the speed) and the ratio of stable to unstable isomers in the PSS (the efficiency). Synthesis of such overcrowded alkenes is not trivial, but can be achieved with the high yielding, though harsh, McMurry reaction.

The symmetrical structure of motor **1** is convenient from a synthetic point of view, but does not allow for easy structural modification. With future applications and surface functionalization in mind, a second generation of molecular motors was designed.

Scheme 12.2 depicts the rotary cycle of second-generation molecular motor **2** [28]. In this class of motors, the upper part is typically referred to as the rotor, while the lower part is called the stator. The rotation proceeds through the same mechanism as for motor **1**. Note that the nonsymmetric stator is essential to unequivocally proof unidirectionality. Without the MeO substituent, stable (*M*)-*E*-**2** and stable (*M*)-*Z*-**2** would be identical, as would unstable (*P*)-*E*-**2** and unstable (*P*)-*Z*-**2**. This would make it theoretically possible for backward rotation to occur unnoticed during THI. Such backward thermal *E*–*Z* isomerization (TEZI) has in fact been observed, but only becomes a competing pathway for THI at higher activation barriers (>110 kJ/mol vs. ~100–105 kJ/mol for the THI's of **2**) [29]. An advantage of second-generation molecular motors is that the activation barrier for the THI is typically very similar for both halves of the rotary cycle, thus ensuring a more regular rotation. As a result, the motor does not require any form of sequential energy input: it will rotate continuously and regularly under continuous irradiation at a constant temperature. For this core structure, the half-life of both the unstable *Z*

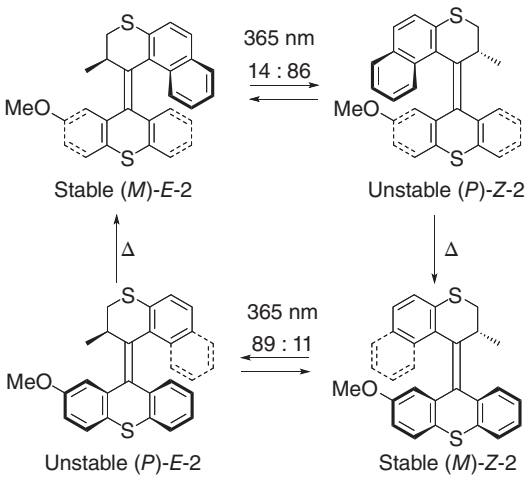

Scheme 12.2 Mechanism of the 360° unidirectional rotation of second-generation molecular motor **2**.

and the unstable *E* isomer is expected to be around nine days [30]. For the synthesis of second-generation molecular motors, the McMurry reaction is less suitable, as it will yield at best a statistical distribution of products. When upper and lower halves have a large size difference, only homocoupled products may be formed. For second-generation motors, the Barton–Kellogg reaction is applied in most cases, and although it requires conversion of the precursor ketones to a thioketone and a diazo compound, it is otherwise usually successful.

A remarkable observation on motor **2** is that a single stereogenic center is apparently enough to create unidirectional rotation. Naturally, this result raised the question whether it would be possible to create a motor without any stereogenic centers.

Such a molecule was realized by merging two second-generation motors, and with that replacing the stereocenter by a pseudoasymmetric center. The rotational process of a third-generation molecular motor is depicted in Scheme 12.3 [31]. Just as for first- and second-generation molecular motors, the thermodynamically favored isomer *meso*-(*r*)-**3** is that in which the largest substituent on the (pseudo)asymmetric carbon (in this case, CH_3) occupies the pseudoaxial position. Upon irradiation with UV light, one of the central double bonds isomerizes, generating a mixture of (*M*)-**3** and (*P*)-**3**. Isomerization of both double bonds at once was not observed. This photoisomerization is followed by a THI, in which the CH_3 substituent moves from a (pseudo)equatorial to a (pseudo)axial position, thus regenerating *meso*-(*r*)-**3**. Similar to second-generation motors with a symmetrical rotor, it is impossible to establish unidirectionality in **3** when R=H. Therefore, a desymmetrized design (R=OMe) was also synthesized and studied, in which the occurrence of TEZI could be excluded. With respect to the core xylene unit, one-half of the motor rotates in a clockwise, and the other in a counterclockwise direction. To the external observer this gives the appearance of both rotors rotating in the same "forward" direction, similar to the wheels on a cart.

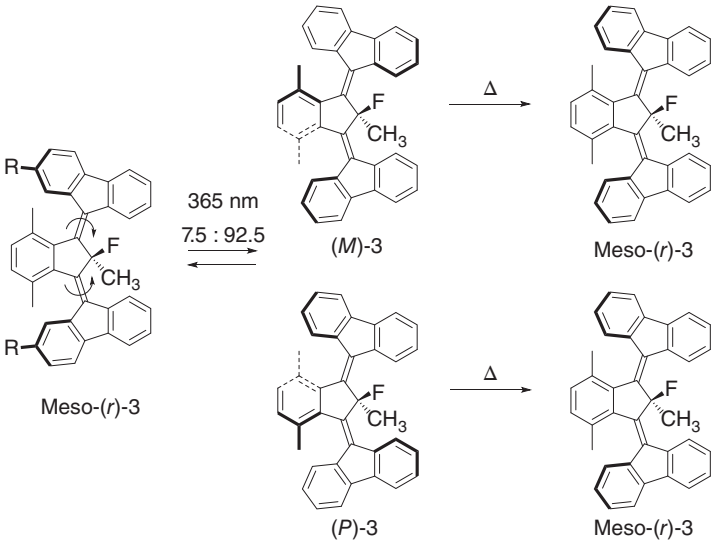

Scheme 12.3 Mechanism of 180° unidirectional rotation of third-generation molecular motor **3**.

12.3 Tuning the Properties of Molecular Motors

While the overcrowded alkene core and chiral elements of molecular motors are crucial for the unidirectional rotation, the structure can be modified in order to tune rotational properties. By far the most extensively explored of these properties is the activation barrier of the THI and consequently the half-life of the unstable isomers. The ability to control the half-life is of paramount importance in the design of responsive systems based on molecular motors. If, for example, the molecule is to be employed as a switch between opposite helicities, raising the activation barrier will prevent unwanted THI occurring. On the other hand, if the actual rotational motion is to be used to fuel a process, an ultrafast motor can be more desirable.

Scheme 12.4 depicts several second-generation molecular motor designs **4–16** that have been reported by our group [28, 33–39], and reveals some trends that need to be considered when designing a motor. In general, a larger upper half in combination with a rigid lower half generates the highest barriers [40]. Molecular motors **13** and **8** may look deceptively similar, but in fact the exchange of the small, rigid five-membered ring and the larger, more flexible six-membered ring results in a factor 5×10^{19} decrease in speed. On the other hand, increasing the size of the substituent at the stereogenic center typically lowers the barrier, as demonstrated by the barrier decrease upon changing the methyl substituents of motors **6** and **7** to *tert*-butyl moieties. These guidelines are however far from iron laws, as certain combinations may lead to unexpected results. For example, decreasing the size of the upper half of motor **5** to generate motor **16** actually increases the half-life of the unstable isomer. A detailed discussion of the relation between speed and structure, supported by density functional theory (DFT) calculations, can be found

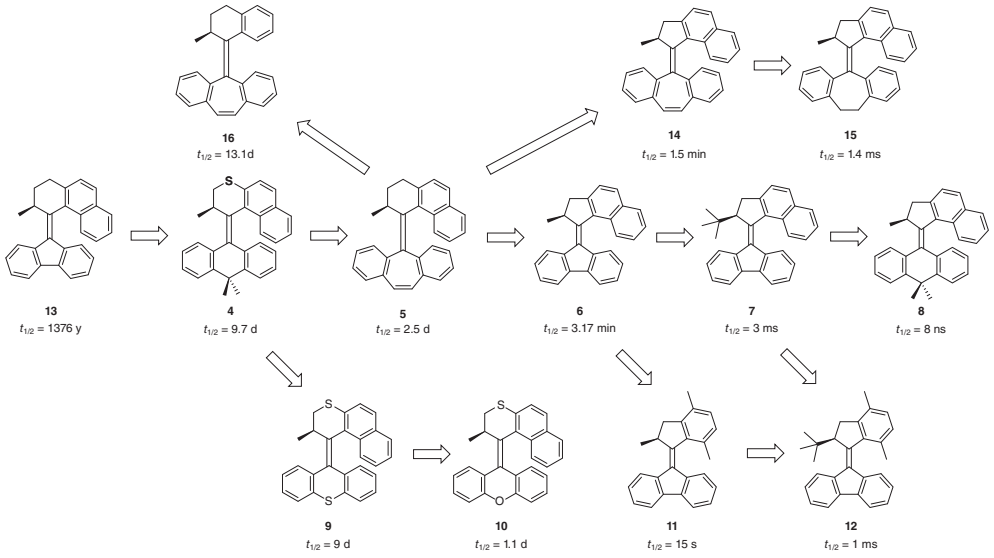

Scheme 12.4 Second-generation molecular motors with increasingly short half-lives. *Source:* Adapted from Chen [32].

in Ref. [40]. It is evident from Scheme 12.4 that even small structural changes may result in very different speeds. This effect was fully exploited in order to modify rotation speed in a dynamic way. Through complexation with different metals, a 4,5-diazafluorenyl-based molecular motor **17** could be slightly contracted so that the speed could be modified up to a factor of 31.5 (Scheme 12.5) [41]. Similar systems allowed for dynamic speed modification via complexation of various alkali cations to a crown ether functionalized molecular motor **18** [42], or hydrogen bonding to a biphenyl-based motor **19** [43]. In addition, gated systems have been developed, in which molecular motor rotation could be switched "on" or "off" through an orthogonal trigger such as acid–base (**20**) [44] or visible light (**21**) [45].

All motors discussed in this chapter thus far operate under UV light irradiation. Shifting the wavelengths toward the visible or even infrared wavelengths is highly desirable in the design of smart materials, as UV light may cause degradation of organic components. For biomedical applications, wavelengths between 650 and 900 nm are considered ideal, while UV wavelengths can cause cell death [46]. Fortunately, several strategies are available to shift the irradiation wavelength of molecular motors toward the visible. Dynamic wavelength shifting was achieved using a Ru(II) complex of the previously discussed 4,5-diazafluorenyl-based molecular motor **17**, which could be rotated with 450 nm light [47]. Even higher wavelengths (530 nm) could be used upon energy transfer from a triplet sensitizer to a covalently attached molecular motor [48]. In addition, several design modifications to the motor core have resulted in red shifting of the absorption maxima. Extending the π system of the aromatic core is a moderately successful approach, but suffers from low quantum yields, and is limited by solubility issues [49, 50]. More effective are push–pull systems, created by installing electron donating and withdrawing substituents on the motor [51, 52]. Finally, recent years have seen the emergence of new types of rotary molecular motor, some of which have strongly redshifted absorption maxima. From our own group come motors based on oxindoles (Scheme 12.6, **22**) [53], which not only can be rotated at higher wavelength but also offer the benefit of easy modular synthesis. The group of Dube has reported molecular motors based on hemithioindigo (Scheme 12.6, **23**) [54], which are very fast and undergo rotation using visible light. While these systems provide access to a greater synthetic diversity, it has to be noted that both rely on the same governing principle as a second-generation motor, i.e. double-bond photoisomerization and THI regulated by an adjacent stereocenter.

The direction of motor rotation is dependent on the chirality at the stereocenter adjacent to the central double bond and is therefore fixed. A single example of a reversible molecular motor has been reported, in which base-catalyzed epimerization of the stereogenic center was used to invert the direction of rotation [55]. However, this system was not fully unidirectional and has found no further application. While there is typically no preference for either clockwise or counterclockwise rotation, for many applications it is necessary that all motors rotate in the same direction. In other words, the motors need to be obtained in enantiopure form. Employing chiral HPLC to separate enantiomers is possible, but not practical when large quantities of material are required. Asymmetric synthesis requires longer synthetic routes, but has been effective.

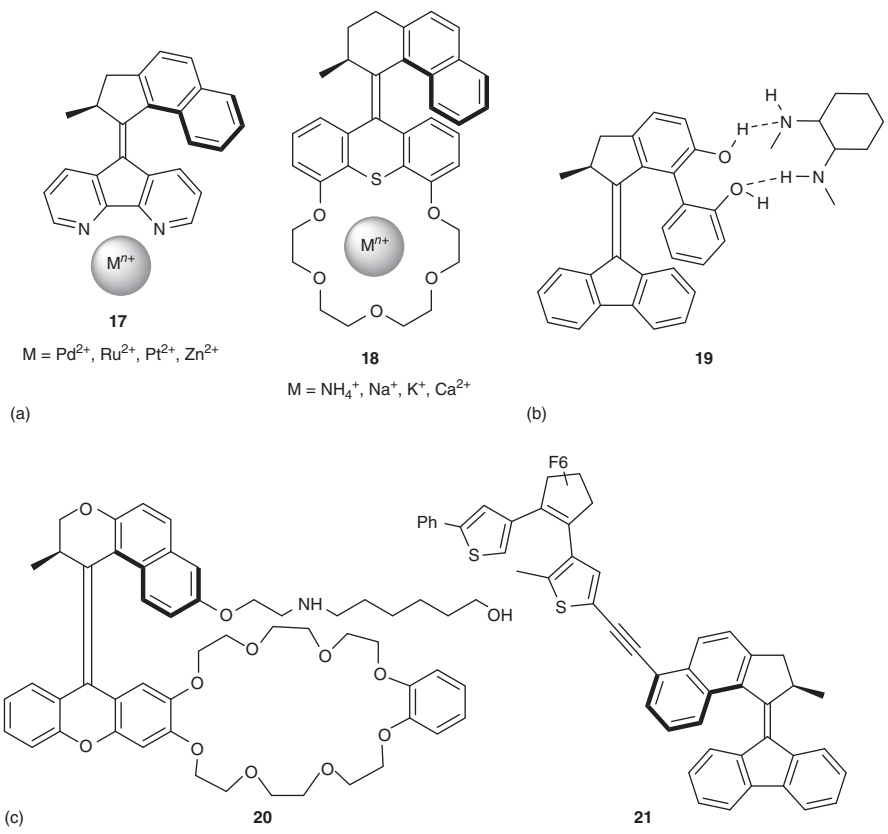

Scheme 12.5 Dynamic speed modification for rotary molecular motors through metal and cation complexation (a, **17** and **18**), hydrogen bonding (b, **19**), and gated systems (c), which can be regulated by addition of acid and base (**20**) or by visible light (**21**). Sources: Based on From Faulkner et al. [41–45].

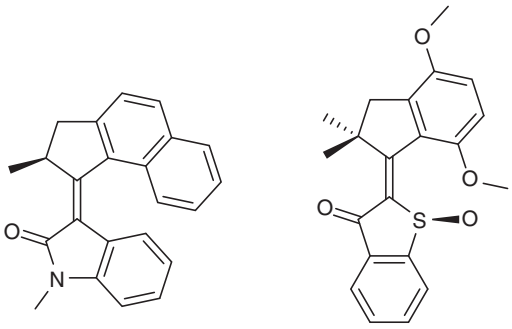

22 23

Scheme 12.6 Oxindole motor **22** and hemithioindigo-based molecular motor **23**.

For first-generation molecular motors, this required development of a modified version of the McMurry reaction, since the standard method involving Zn and $TiCl_4$ induces partial racemization of the stereogenic α center [56]. For second-generation molecular motors, a Barton–Kellogg reaction is typically used to couple the upper and lower halves. Conversion of the precursor ketone into the required thioketone or hydrazone causes racemization, which can be prevented if the β position is also methylated [57]. Second-generation molecular motors containing hydroxy or methoxy substituents at the asymmetric carbon can also be synthesized enantiomerically pure, but do not show completely unidirectional rotation [58, 59]. At the moment, the best results have been obtained using chiral resolution. Our group reported that a hydroxyl functionalized first-generation molecular motor can be obtained in >99% ee via co-crystallization with chiral *N*-benzylcinchonidinium chloride [60]. Remarkably, the resolving agent preferentially binds the (*R*,*R*)-enantiomer in ethyl acetate, while the (*S*,*S*)-enantiomer was preferred in acetonitrile. Recently, the group of Giuseppone reported a game-changing method of synthesizing enantiomerically pure second-generation molecular motors [61]. By functionalizing the racemic upper half with chiral auxiliaries, the diastereomers of the motor can easily be separated on a standard achiral silica column. As a result, the motor could be synthesized on a 755 mg scale, providing quantities that offer potential in smart material design. Additionally, the motor has orthogonal functional groups at the upper and lower halves, which may easily be further derivatized.

12.4 Molecular Motors as Out-of-Equilibrium Systems

Grzybowski and coauthors state that "molecular machines, in sharp contrast to switches, should be able to drive multifarious chemical reactions uphill and away from their 'inherent' equilibria" [62]. Before considering the different strategies toward amplifying motor function in order to generate work, it is important to answer the question whether rotary molecular motors qualify as molecular machines and cast a detailed look at the requirements for out-of-equilibrium systems.

In order for a system to operate away from the thermodynamic equilibrium, a constant energy input is required. A molecular photoswitch is a molecule that can undergo a structural change upon exposure to light [63]. Through photoexcitation and subsequent relaxation, the molecule can reach a higher energy metastable state that cannot be reached in thermal equilibrium. Depending on the height of the barrier for the downhill reaction, the molecule may be able to return to the initial state thermally. A photochemically driven backward reaction may also occur, as it is often not possible to excite one of the two isomers selectively. If thermal and/or photochemical backward movement is possible, irradiation will lead to the formation of an equilibrium in which forward and backward rates are in balance and in which part of the population resides in the metastable state. Sustaining this equilibrium (or PSS, *vide supra*) requires continuous energy input. If irradiation is stopped, conversion between the two states will be halted, and in case of a sufficiently low barrier, all molecules will thermally revert to the initial state.

Although a system at PSS clearly operates away from the thermal equilibrium, the output generated by a photoswitch is reversible – any work done is subsequently undone. In order to perform work, the movement needs to be performed directionally and repetitively [14]. Fortunately, the work performed by molecular switches can be harnessed through a ratcheting mechanism [62]. The molecular motors described in this chapter are essentially overcrowded alkene switches, and the initial establishment of a PSS (for example, between stable *E* and metastable *Z*) can easily be recognized as the photochemical equilibrium described here for photoswitches. However, the introduction of a stereocenter adjacent to the rotary axle causes a desymmetrization of the energy landscape. From the metastable state, the molecule can reach a second thermodynamic minimum (stable *Z*) through forward THI. The barrier for the forward process is much lower than for thermal back isomerization; thus, backward movement is effectively blocked. If the sequence of photochemical isomerization and THI is repeated, the stable *E* isomer is regenerated. However, it is important to note that this does not imply that the work performed by the motor is undone – the motor has completed a full 360° rotation. The isomer at the newly reached minimum, although structurally identical to the initial stable *E*, is therefore most accurately referred to as stable *E*′. Due to the aforementioned desymmetrization of the energy landscape, maintaining a photochemical equilibrium as described for photoswitches is not possible for rotary molecular motors. Instead, some thermal isomerization will lead to formation of the other stable isomer, which may also undergo photoisomerization. Therefore, at the photogenerated stationary state for rotary molecular motors, all four states are populated. This state operates away from equilibrium, since stopping the irradiation will lead to a gradual disappearance of the metastable states via THI. Additionally, the system performs work, as the interconversion between the different isomers occurs only through the unidirectional rotation cycle. In conclusion, there is a distinct difference between the operation of a ratchet and a power stroke machine [64–66].

Before starting our discussion on out-of-equilibrium systems based on molecular motors, we have to remark on a practical matter, relating to temperature.

Light-driven rotary molecular motors are – although the name may suggest otherwise – of course not only driven by light. Without the THI step, these molecules would simply function as complicated bistable photoswitches. The presence of a thermal process in the rotational cycle has far-reaching consequences with respect to the population of the various states at different temperatures. The question therefore arises what the out-of-equilibrium state for a molecular motor actually looks like. If a system is operated at a temperature where the half-life of the metastable state is more than a year, are we not observing a bistable photoswitch? If the half-life of the metastable state is so short it can't be observed, are we not looking at an equilibrium between two stable isomers at the thermal minimum? These questions are not easily answered, and are perhaps mostly of a philosophical nature. In this chapter, we simply consider systems at the temperature at which they are operated and their limits of practical use. An ultrafast motor is able to perform work because all components pass through the metastable states – no matter how short lived. An ultraslow motor is not, if it is expected to degrade long before a measurable amount of work can be performed.

12.5 Single Molecules Generating Work on the Nanoscale

Based on any standard definition of the term [8, 14, 62, 67], every light-driven rotary molecular motor performs work, i.e. converts light and heat energy into rotational motion. However, to fully exploit the potential of these machines, the rotational motion generated by the motor should be transferred into yet another form of energy, such as translational motion or mechanical work. Although the work generated by a single molecule appears negligible at the macroscale, it should not be overlooked that each individual molecule is a functional machine in its own right. A few selected examples beautifully demonstrate the potential of molecular motors to fuel future nanomachinery.

Following some initial exploration by the group of Tour [68–71], in 2011 our group reported the first functioning example of a motorized molecular nanocar **24** (Figure 12.1a) [72]. This molecule, much like a regular car, is designed in the shape of central chassis connecting four wheels: second-generation molecular motors. After sublimation on a copper surface, aScanning Tunnelling Microscopy (STM) tip was used to apply an electric pulse to the nanocar **24**, thus inducing movement. By performing 10 of these steps consecutively, a single molecule managed to complete a 6 nm long linear trajectory. Although in this example an electric voltage is used to fuel the motors instead of light irradiation followed by thermal relaxation, the motors appear to undergo the same rotational process. Thus, this molecular machine does not only convert its energetic input into rotational motion of the motor wheels but also converts this rotational energy into directional movement of the entire molecular car. As such, this publication constitutes a landmark in the history of light-driven molecular motors as the first (and to this date, one of a few) example in the which the motor was not used to switch between states, but to

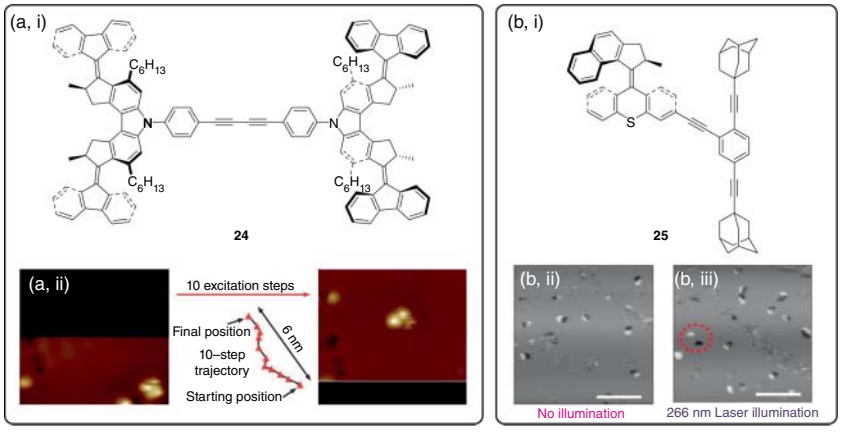

Figure 12.1 (a) Structure of a motorized nanocar (i) and the 6 nm trajectory it completed on a gold surface (ii), including STM images of the starting (left) and finishing position (right). (b, i) Structure of the "nanoroadster," (ii) difference images of the roadsters at their starting positions (dark) and after thermally induced diffusion (white), and (iii) difference images of the roadsters at their starting positions (dark) and after irradiation with a 266 nm laser (white). *Source:* Figures adapted with permission from references Kudernac et al. [72] (copyright 2011, Springer Nature) and Saywell et al. [73] (copyright 2016, American Chemical Society).

drive a process by consecutive unidirectional rotation, and address the fundamental challenge of converting rotary motion into translational motion.

Recently, Tour and coworkers [73] reported a so-called "nanoroadster" **25** (Figure 12.1b). This molecule consists of a second-generation molecular motor connected to an axle containing two adamantane wheels. Although no directional movement was observed, rotation of the motor induced an increased speed of diffusion of the roadsters on a copper surface.

The ability of a molecular motor to generate nanomechanical force was spectacularly demonstrated by Tour and coworkers [74], who utilized them as nanoscale drills disrupting a cell membrane. Upon irradiation, modified motors that are not toxic under nonirradiation conditions cross the cell membrane and induce apoptosis. Modification with small peptides allowed for specific cell targeting. A follow-up publication utilized motors that can be rotated using visible light, this avoiding UV-light-induced cell death [75].

12.5.1 Molecular Stirring

When a molecular motor rotates in solution, the rotational energy is dissipated. The effect of this energy on the environment can also be considered as a form of work and has been studied in detail. As the motor rotates, a rearrangement of the solvent shell is required. Viscosity is a complex interplay of intermolecular interactions, but it quite simply follows that the higher the viscosity, the more difficult it is to rearrange the solvent shell and therefore for the motor to rotate [76, 77]. In other

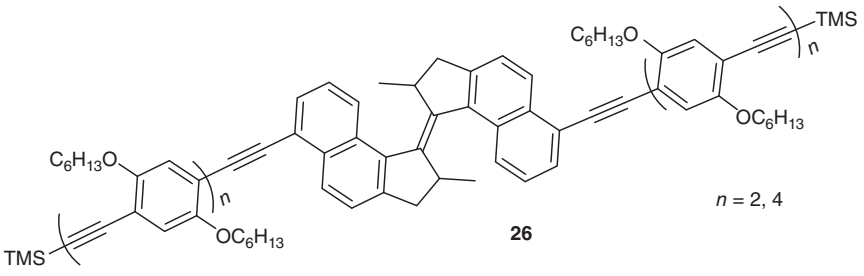

Scheme 12.7 Structure of molecular stirrer **26**. *Source:* From Chen et al. [78].

words, a faster and more powerful motor will cause more rearrangement of the solvent shell, thus performing more work.

The capacity of a molecular motor to create a disturbance in its environment was explored with the design of a molecular stirrer **26** (Scheme 12.7) [78]. This first-generation molecular motor was functionalized with long, rigid substituents, specifically to create a maximal disturbance in solution. Contrary to a previous design with alkyl chains, which proved to have the same rotation speed as its unsubstituted parent compound [79], the "rearranging volume" was increased 24-fold compared with the parent motor. In a highly viscous medium, the half-life of the molecular stirrer was more than two days at room temperature, compared with nearly three hours for the parent. Therefore, it can be stated that the rigid substituents act as paddles disturbing the solvent shell, slowing down the motor as they do so. This model was supported by DFT calculations and found to be in accordance with the free volume model [80]. Theoretically, the work done could be harnessed – by continuous rotation one could generate high diffusivity and as such increase reaction speed. In practice, disturbance of the solution shells appears to be extremely local, and rotation speed is limited by the amount of light that can be supplied to the system. Up until now, no increase in solvent diffusivity has been demonstrated.

Tour and coworkers [81] took a different approach toward investigating the work exerted on the environment by a molecular motor. The core of their unimolecular submersible nanomachine (USN) **27** (Scheme 12.8) consists of a previously reported second-generation molecular motor, which has a half-life in the nanosecond regime [33]. This motor was functionalized with two Cy5 fluorophore moieties and investigated using confocal fluorescence microscopy in acetonitrile. It was observed that under UV irradiation, the diffusion speed of the USN increased by 26%. The authors state that rotation of the motor moiety propels the USN through solution with a step size of 9 nm per rotation, thus effectively speeding up diffusion, although no mechanism of this enhanced movement is proposed.

12.5.2 Amplifying Motor Function

The versatility of light-driven rotary molecular motors derives from the combination of processes that together make up the unidirectional rotation cycle. In addition to

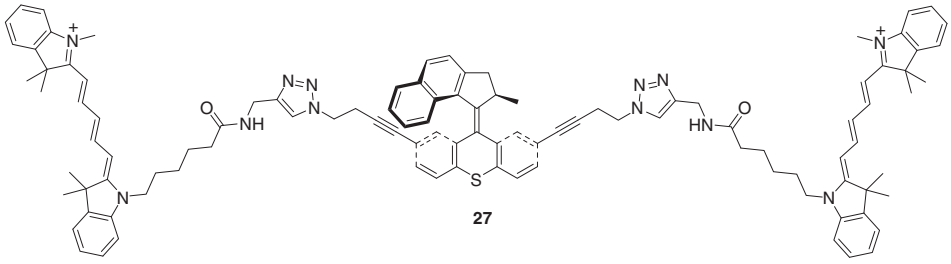

27

Scheme 12.8 Structure of unimolecular submersible nanomachine **27**. *Source:* From García-López et al. [81].

the continuous unidirectional rotation, rotary molecular motors display two other dynamic properties that can be utilized. First of all, since both light and heat can be applied with high precision, molecular motors serve as advanced four-state switches. Both photochemical steps are reversible, making molecular motors also a type of bistable molecular photoswitch in temperature ranges where THI is negligible. Secondly, the overcrowded central double bond ensures that rotary molecular motors are helical. While the stereochemistry at the carbon adjacent to the double bond is fixed and determines the direction of rotation, the helicity of the whole molecule is inverted in every photochemical and thermal step. This light-responsive change in chirality has found application in photoswitchable multistep catalysis [82].

Having now established that molecular motors operate away from thermal equilibrium and are able to perform work, the next challenge is to amplify this work on the nanoscale to micro- or macroscale work performed by responsive smart materials based on molecular motors. In other words, the unidirectional rotation of the motor needs to be applied. However, creating such materials is an area of research that is still in its infancy, and arguably only a handful of applications that can truly be identified to truly perform work have been reported. Meanwhile, several approaches toward amplifying and harnessing molecular motor switching have been developed, which can prove instructive in the design of larger out-of-equilibrium systems. Effectively, creating a micro- or macroscale effect from collective motor motion requires overcoming Brownian motion by overcoming random movement and enforcing order to generate a collective effect. In the remainder of this chapter, we will assess the three main strategies toward amplification of motor function, highlight them using examples from literature, and if applicable, discuss the non-equilibrium characteristics of the system.

- Immobilization of the molecules to induce positional and orientational order and harness their rotation either on surfaces and monolayers or in 3D networks, like polymers or metal organic frameworks.
- Doping of polymeric or liquid crystalline materials, in which the intrinsic helicity of the motor is exploited by inducing a responsive chirality of the doped system as a whole.
- Self-assembly to form responsive materials based mainly on amphiphilic structures.

12.6 Immobilization

12.6.1 Surface-Attached Molecular Motors

When operated in solution, molecular motors show neither positional nor orientational order, which makes it difficult to harness their cooperative rotation and perform useful functions. Surface immobilization is one of the possibilities to overcome Brownian motion and give an opportunity to turn the relative rotation of one motor half with respect to the other into an absolute rotation of the motor with respect to the surface [83].

When attached to the surface, molecular motors can either have an azimuthal [83–88], rotating parallel to the surface (Scheme 12.9, **28**), or altitudinal [89–93] orientation, with the rotor oriented perpendicular to the surface (Scheme 12.9, **29**).

The first examples of surface mounted motors have been realized in an azimuthal orientation on gold nanoparticles [83]. The lower half of the motor is connected to the metal through thiol groups with two "legs" as points of attachment. The use of multiple attachment points prevents the free rotation of the motor molecules with respect to the surface while maintaining the functioning of the motor. To bypass quenching of the excited state by the gold before isomerization, the motors need to have a large distance from the surface. The increased length of the tethers comes at the cost of a decreased rigidity of the system, because the molecules have the freedom to lie flat on the surface, hampering their ability to perform the motor rotation. Furthermore, the nature of the tether should provide the motor with enough space to rotate freely and not be blocked by neighboring molecules. Most systems with bipodal attachments suffer from decreased freedom of rotation of the rotor on the surface compared with the solution because of a lack of free volume, resulting in an increased half-life [84–86, 89, 90]. To some extent, dilution and formation of mixed monolayers and therefore attachment of fewer motors on the surface allow the free rotation of the molecules [93], but a careful design of the tether is more effective.

The noncovalently attached bipodal motor **30** recently reported by our group overcomes these difficulties (Scheme 12.9, right) [88]. The motor is equipped with four carboxylate groups, which bind with an amine-coated quartz surface. The half-life of the thermal isomerization step of 161 seconds is comparable with that reported in solution (130 seconds), which indicates that the motor has enough free space to rotate due to a bulky linker for attachment. A derivative with only two carboxylate groups on the lower half of the motor has a significantly longer thermal half-life on the surface (3855 seconds) compared with solution (227 seconds), indicating that the carboxylate groups are crucial in providing free space for the motor rotation.

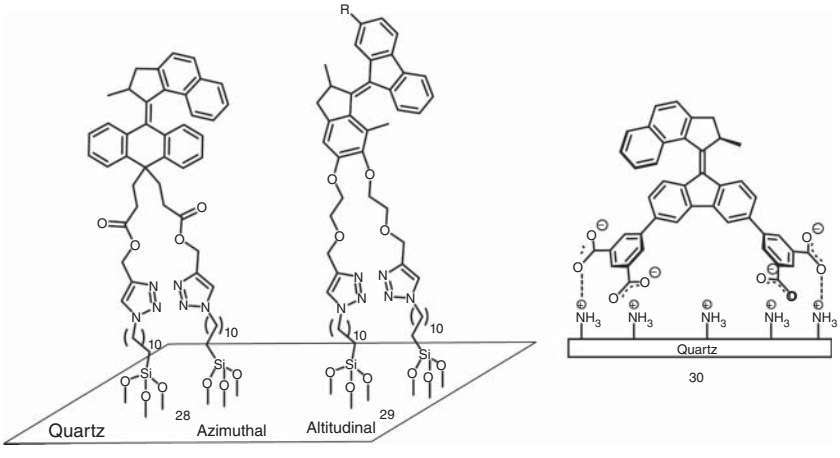

Scheme 12.9 Examples of surface-mounted molecular motors in azimuthal (**28**) and altitudinal (**29**) orientations, and attached via noncovalent interactions (**30**).

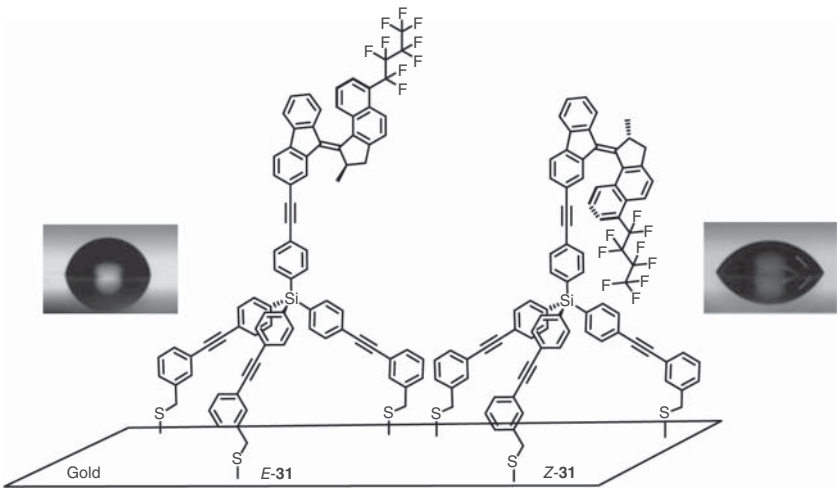

Figure 12.2 Tripodal molecular motor for surface attachment in self-assembled monolayers on a gold surface. Top: molecular structure, showcasing the dynamic hydrophobic moiety. Bottom: water droplet on a stable *Z*-SAM (left) and stable *E*-SAM (right). *Source:* Adapted from Ref. Chen et al. [92]. Copyright 2014, American Chemical Society.

In contrast to the azimuthal orientation, the altitudinal orientation offers the opportunity to expose or hide away a functionality on the rotor part of the system from the surface upon motor rotation and as a result change the surface properties. Figure 12.2 depicts a recent example of a surface-immobilized altitudinal motor **31**, which was mounted via three sulfide bridges on a self-assembled monolayer (SAM) on a gold surface [92]. The so-called tripod was functionalized with a perfluorinated moiety at the rotor part in order to observe a change in surface wettability upon rotation of the molecule. The bulky nature of the tripod provides sufficient free volume for the motor to rotate without restriction and keeps enough space between motor and surface at the same time. The half-lives of the thermal isomerization steps on the surface ($t_{1/2} = 530$ seconds for unstable Z to stable Z and 351 seconds for unstable E to stable E) gave similar values as in solution ($t_{1/2} = 402$ seconds for unstable Z to stable Z and 307 seconds for unstable E to stable E). A significant change of surface wettability was observed upon irradiation of the surfaces, demonstrating the possibility to achieve macroscopic effects through the collective movement of multiple molecules in the confinement of the surface. However, the reversibility of the switching is limited, due to the low PSS of the mounted motors.

Photochemical and thermal isomerization are not compromised by the confinement of molecular motors with long hydrophobic rods in a surface inclusion complex with the hexagonal porous structure of tris(*o*-phenylene)cyclotriphosphazene, as demonstrated by our group in collaboration with the groups of Michl and Kaleta [94]. For these motors, precisely spaced at 1.1 nm, the rotation is not

hampered even when the surface is fully covered. Therefore, this highly ordered noncovalent system offers ample opportunities for future modular surface functionalization and synchronizing motion.

12.6.2 3D Networks

A fairly recent approach to immobilization of molecular motors is their incorporation in polymer networks. Polymer chains are covalently attached to the upper and lower half of the molecules, and they therefore act as a novel kind of responsive cross-link unit to form polymeric organogels. This undermines the free movement of the motor, and thus the rotation can be transferred onto the polymer network upon irradiation.

A remarkable example using this approach was presented by the group of Giuseppone in 2015 (Figure 12.3) [95]. The synthesis of the core unit, inspired by structures developed in our group [39], was adapted to allow for gram scale synthesis [61]. The introduction of two chiral groups in the upper half of the molecular motor allowed diastereomeric separation of the *R* and the *S* isomer of the molecular motor and the synthesis of a material with enantiomerically pure motors. The synthesis of the polymer was concluded by supplying the molecular motor with alkyne-terminated long ethylene glycol chains and subsequent cross-linking of the motor units by a copper catalyzed click reaction (Figure 12.3, left). The product of the final reaction depends on concentration; an eight-shaped single cross-linked molecular motor is obtained for low concentrations of the precursor in solution (Figure 12.3, middle), while high concentrations result in a complex network of multiple cross-linked motors (Figure 12.3, right).

Upon irradiation of the cross-linked polymeric gel with 366 nm light at room temperature, the motor starts rotating and entangles the polymer chains as a result. This leads to a contraction of the polymeric gel of up to ~80% (Figure 12.3, right) until

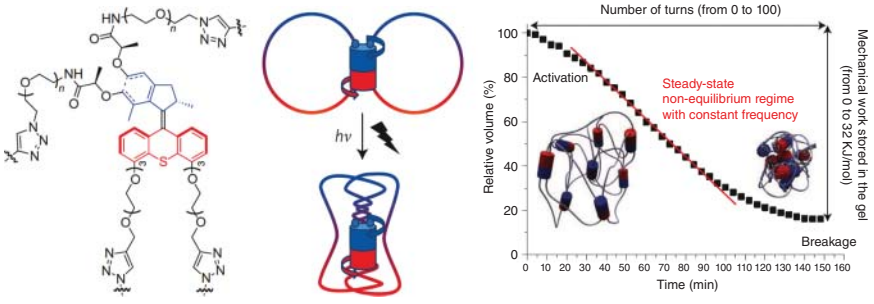

Figure 12.3 A motorized polymer gel. Left: structure of the motor core unit. Middle: Figure-of-eight structure formed at low concentrations. Right: Macroscopic behavior of the gel upon irradiation, over time, and graphic representation of motorized polymer network obtained at high concentrations. *Source:* From Li et al. [95]. © 2015, Springer Nature.

rupture occurs, recovering the original shape and volume of the material. The sudden rupture arises from the breaking of the central double bond of the motor through its increased reactivity toward oxidation upon strain. The motor halves stay connected through a single bond; thus, the functionality of the material is lost while its topology stays intact. Therefore, the contraction of the gel cannot be undone without chemical modification, which reduces the functioning of the material to a onetime event. Hence, the far-from-equilibrium operation of the system is limited to the point at which the material breaks, and the energy input through light irradiation cannot be dissipated endlessly. Regardless, this publication represents a landmark on the road toward generating macroscale work from molecular motion. In addition, the importance of new synthetic route toward gram quantities of enantiopure molecular motor cannot be underestimated for smart materials design.

The limitations of Giuseppone's system were addressed by the same group in an extension of their approach by incorporating modulators in the gel [96]. In addition to the motor cross-links, dithienylethene cross-links were added to the polymer network, acting as a strain releaser operating on another wavelength than the molecular motor. Upon irradiation with UV light, the motor rotation is induced, and the modulator will stay in its closed conformation, sustaining the strain buildup by the torsion of the polymer chains. Upon subsequent irradiation with white light, the dithienylethene adopts its open form, and the accumulated strain of the braided polymer chains can be released as kinetic energy through free rotation of the formed C—C single bonds. The gel nearly regains its initial volume within multiple hours of irradiation. Simultaneous irradiation of the polymer with UV and white light induces both the winding and the unwinding to proceed concurrently. The constant influx of energy is dissipated through the movement of the polymer chains through the photoactive cross-linkers within the network. However, when observing the material from the outside, no macroscopic change can be observed in this photogenerated equilibrium. The work that is performed by the motor with entangling the polymer chains is simply undone by opening of the modulators.

Another interesting approach to incorporating molecular motors in a solid, polymerlike network was presented recently by the group of Feringa [97] (Figure 12.4). Pyridine functionalized molecular motors were incorporated in a coordination polymer, or molecular organic framework (MOF) [98–103] together with 1,4-dibromo-2,3,5,6-tetrakis(4-.carboxyphenyl)benzene (TCPB) allowing their well-defined spatial organization within a solid material and potential to display collective rotational movement. MOFs are rigid porous structures with an architecture defined by the building blocks used to synthesize them. Their network offers enough free volume within its pores for the motor to retain its rotational movement unhindered in the solid state [97, 102].

The material chosen was a zinc-pillared paddlewheeled MOF. Within the network, zinc ions function as cornerstones for a tetracarboxylic acid linker, which organizes as layers separated by bipyridine-functionalized molecular motors as pillars in

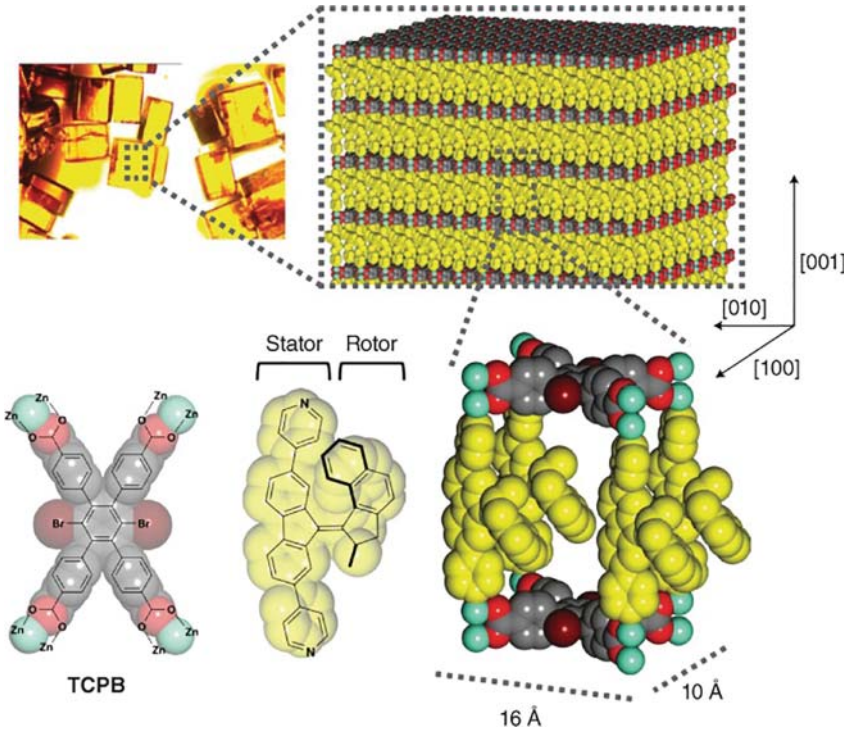

Figure 12.4 Motorized metal–organic frameworks (moto-MOFs). Schematic representation of the 3D organization within the framework, and dimensions and representation of a single cell. *Source:* Source: From Danowski et al. [97]. © Springer Nature.

the third dimension. The motor was incorporated through a solvent-assisted linker exchange (SALE) [104], swapping a dipyridyl–naphthalenediimide linker with a 4,4′-bipyridine-functionalized motor. This strategy allowed for incorporation of the motor under milder conditions than in a *de novo* synthesis of the MOF, which was expected to result in the decomposition of the motor.

Comparing the rotational behavior of the motor in solution and in the solid state, it was demonstrated that the rotation takes place without hindrance. Similar values for PSS and rotational speed are obtained compared with the solution state, as confirmed by Raman spectroscopy. Once the light source is removed, THI occurs, and the motor completes its rotation and adapts its stable state. No fatigue was observed upon long-term irradiation and repeated rotation cycles.

These results nicely demonstrate the MOFs potential to achieve precise organization of molecular motors in a solid bulk material. In order to further improve the material, it will be necessary to enforce orientational order of the motors additionally to the already achieved positional alignment, qualifying it, for instance, for the applications such as transport processes through the pores of the network as a result of the collective rotational movement of the motors.

12.7 Liquid Crystals and Polymer Doping

Amplification of chirality from small molecules to a macromolecule or a supramolecular system has been fascinating researchers on their quest of finding the origin of homochirality in nature [105, 106], as it is observed in the formation of complex self-assembled structures like DNA [106]. In addition, this research field has more application-based interests, such as developing new materials that can be applied in information storage, smart films, and sensing [107, 108]. With the use of small molecule dopants, chiral information can be transferred and amplified in, for example, chiral gels [109–111], helical polymers [112, 113], and liquid crystals (LCs) [114–116]. Additionally, bistable dopants that can be controlled using stimuli such as light and heat facilitate the control of a material in a dynamic and reversible manner. The potential and application of molecular motors for this purpose is evident from the intrinsic change in chirality upon light irradiation. In this chapter, we discuss the work that has been done on the amplification of the motors chirality using supramolecular and polymeric systems.

12.7.1 Liquid Crystals

LCs are a unique class of materials that adopt a state of matter between the liquid and the solid phase, called the mesophase [115]. In the liquid crystalline state, the molecules, or mesogens, weakly interact and therefore organize to a certain degree, but less than in a crystalline material. Hence such substances possess properties of both liquid and crystalline materials. This combination of stable intrinsic order despite their weak, dynamic intermolecular interactions puts LC in a unique position for the widespread application in sensors, information storage, smart films, and LC displays. Furthermore, they can be regulated using multiple different stimuli, like temperature or electric fields or the incorporation of non-mesogenic molecules within the liquid crystalline matrix.

LC can be divided in several distinct categories. The most simple LC are nematic LC, in which the mesogens adapt a parallel orientation, but are not arranged in phase. In contrast, chiral nematic or cholesteric LC are oriented parallel and additionally take on a helical structure and are therefore organized in a chiral assembly. The supramolecular chirality of these structures is described by the cholesteric pitch (p), which is defined as the distance in which the helix completes a full 360° rotation. Chiral dopants dissolved in the LC matrix can induce a cholesteric phase in a nematic LC. The pitch strongly depends on the nature of the dopant. The efficiency with which the dopant induces the helicity within the assembly is called helical twisting power (β). That value is intrinsic for every LC-dopant combination and is a reflection of the amount of dopant needed to reach a cholesteric phase with a certain pitch. The pitch is hence inversely proportional to the concentration, the enantiomeric excess (ee), and the helical twisting power of the dopant. A strong resemblance between mesogen and dopant often proves to be beneficial for good solubility of the guest and therefore a strong host–guest interaction (Figure 12.5):

$$p = [\beta(ee)c]^{-1} \tag{12.1}$$

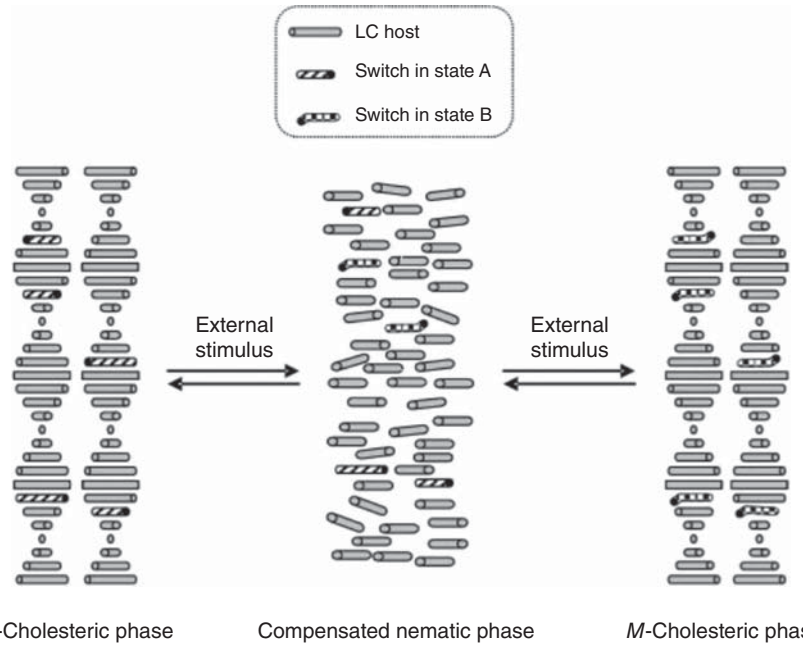

Figure 12.5 Dynamic conversion between LC nematic and cholesteric phases. *Source:* From Eelkema and Feringa [115]. © 2006 Royal Society of Chemistry.

The use of chiral dopants to induce chirality in LC is a successful strategy, which has been exploited in a number of different systems. The pitch can be easily tuned by variation of the ratio of dopant to mesogen. Both LC and dopant can be synthesized separately and combined post-synthetically. Bistable dopants furthermore offer the possibility to control the supramolecular chirality of the LC material using external stimuli, such as light or heat. Light is the more favorable option, since it offers a higher spatiotemporal resolution; can easily be used with different wavelengths, intensities, or polarizations; and most importantly can specifically address the dopant within the matrix without having too much influence on the system as a whole.

Overcrowded alkenes are particularly interesting candidates for inducing cholesteric phases in nematic LCs [117, 118]. They typically have high helical twisting powers, and their intrinsic chirality can be inversed through photoisomerization. An early example presented by the group of Feringa was based on a chiroptical switch with a tertiary hexyl amine to enhance the interaction of the dopant with the LC matrix used (4′-(pentyloxy)-4-biphenylcarbonitrile, **E7**) (Scheme 12.10). Addition of enantiomerically pure dopant (*P*)-*Z*-**32** led to the formation of a chiral nematic LC with *P* helicity and a pitch of $-10.1\ \mu m^{-1}$. Dissolving (*M*)-*E*-**32** in the LC matrix induces the opposite helicity in the material with a pitch of $-13.5\ \mu m^{-1}$.

Although quantitative switching could not be achieved in this system, irradiation of a sample of (*M*)-*E*-**32** (2.6 wt%) in the LC matrix using 380 nm UV light lead to a PSS containing 23% *P* and 77% *M*. Irradiating with 465 nm light resulted in a PSS containing 87% of *P* and 13% of *M*. Reversible switching of the dopant helicity

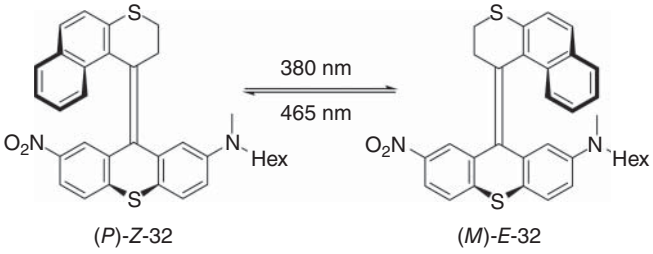

Scheme 12.10 Chiroptical switch designed for enhanced LC doping interactions.

with 380 and 470 nm therefore results in modulating the pitch between −5.1 and $+5.5\,\mu m^{-1}$.

In an effort to proceed from a bistable to a more dynamic system that can operate outside of the thermodynamic equilibrium, an LC was doped with a first-generation molecular motor [119]. It was demonstrated that the motor retains its ability to perform repetitive unidirectional rotation in the LC matrix. The movement of the motor induced a dynamic color change of the LC film through the whole color spectrum upon light irradiation. Visible light is reflected by the cholesteric LC, when the length of the helical pitch is in the same range as the wavelength of the light that is being reflected. Upon irradiation with 280 nm light, the color of the LC shifts bathochromically from violet all across the color spectrum to red, in a matter of seconds. Heating the system to 60 °C reverts the process and induces a hypsochromic shift, indicating that THI occurs, which drives the system forward, reassuming *P* helicity.

A fully light controlled color change without the need to heat the system was accomplished, when a second-generation motor was used for incorporation into the LC host [116]. The fluorene lower half of the molecular motor has a strong resemblance to the mesogen's biphenyl core and therefore a stronger interaction with the LC matrix. Second-generation motors proved to have much higher helical twisting powers in both their stable ($90\,\mu m^{-1}$) and unstable ($-59\,\mu m^{-1}$) forms with a fully reversible and complete helicity inversion of the cholesteric phase in the LC upon irradiation. With the change of helical twisting power of the dopant upon light irradiation, the pitch of the LC changes and with it the supramolecular assembly. A major breakthrough was achieved when the same host–guest system was used to rotate microscale objects (Figure 12.6) [114, 120]. The motor dopant rotation causes stress in the confinement of the LC in a thin film, which is released through reorganization of the molecular assembly. This induces a change of surface orientation in the polygonal fingerprint texture on the surface of the film. This movement can be transferred onto a microscale object (like a glass rod), when it's placed on top of the film. The rotation of the rod under irradiation continues until the system has reached its PSS. Afterward the movement halts, and only continuous UV irradiation ($\lambda = 365$ nm) can maintain the assembled steady state the system is in. When the light irradiation is stopped, the dopant falls back into its stable form through a THI. As such, the whole assembly relaxes and assumes its original configuration by rotating in the opposite direction. This means that the rotation of

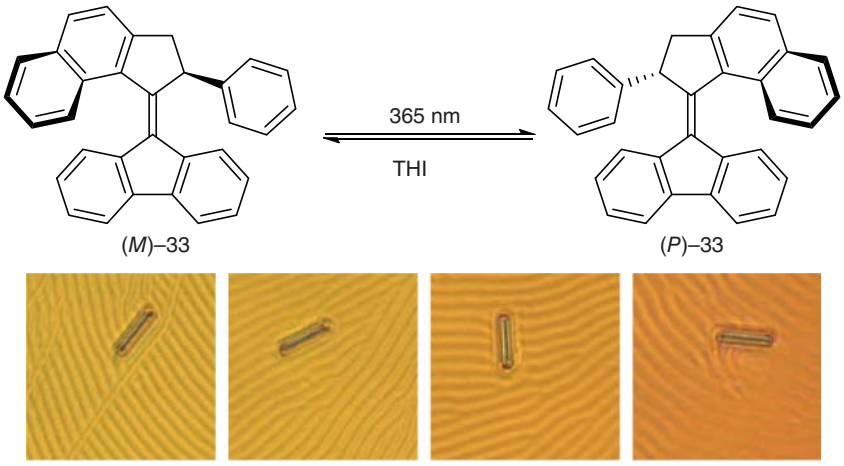

Figure 12.6 Structure of motor dopant **33** (top) and glass rod rotating on the LC surface upon irradiation with 365 nm light (bottom). Frames (from left) were taken at 15 seconds intervals. *Source:* Reproduced with permission from Ref. Eelkema et al. [114]. Copyright 2006, Springer Nature.

the rod reflects the change in chirality of the motor, instead of directly following its rotational movement, indicating that there is no direct transmission of the motor rotation to the microscopic rotation. As a result, the amount of work the system can perform is limited up to the point when the motor reaches PSS. The work performed gets undone upon removal of the energy source.

However, not only does this work demonstrate how the rotation of the molecular motor can be actuated in a molecular assembly to move objects 10 000 times their own size, despite only making up 1 wt% of the mixture. It also serves as an example for a supramolecular system away from equilibrium, since a continuous energy input is needed at the PSS to keep the assembly in the state that it is in. Once the light as the energy source is removed, the system returns to its stable state. A more recent study extended this approach to LC droplets [121].

In 2018, Katsonis and coworkers [122] report the integration of motor **33** in LC E7 together with 1,'1-bi-2-naphthol (BINOL) as a passive co-dopant. Confinement between two glass slides and locally focused irradiation with a laser beam enables rotational movement of the LC through movement of the chiral dopant. In this case the motors are capable of diffusing away and to the area of irradiation, facilitating the operation of the system away from thermal equilibrium. Small LC like cargos were transported in a circular motion along the movement of the motor-doped LC matrix. By a clever manipulation of the system, the group was therefore able to generate an oscillating pattern from continuous illumination. As such, the out-of-equilibrium properties of molecular motors were efficiently translated to the micrometer scale.

12.7.2 Polymer Doping

Polyisocyanate is a rigid, liquid crystal forming polymer, which adopts a helical conformation in solution. *P* and *M* helical polymers exist in equal amounts and are in

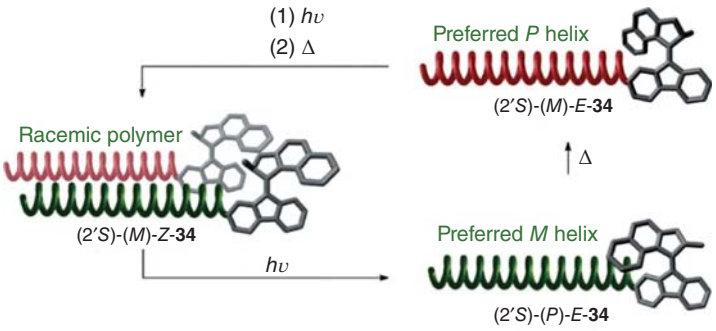

Figure 12.7 The helicity of the second-generation molecular motor **34** can be transferred onto a covalently attached polyisocyanate chain. Under constant light irradiation the motor undergoes a continuous rotation, constantly isomerizing between *M* and *P* helicity. *Source:* From Pijper and Feringa [113]. © John Wiley and Sons.

rapid equilibrium. Due to the strong cooperativity between the achiral monomers, a small change in the structure, as simple as an exchange of a hydrogen atom for a deuterium atom [123], can result in a high preference for one helical sense over the other. In the systems described in this paragraph, the intrinsic chirality of the motor is used to dynamically influence the helicity of these polymer chains.

An enantiopure second-generation molecular motor **34** was modified for use as an initiator for polymerization of hexylisocyanate (Figure 12.7) [113]. As a result, each long poly-(*n*)-hexylisocyanate chain contains a single molecular motor at the terminal position. For the (2′*S*)-(*M*)-*Z*-**34** isomer, no preference of helicity of the polymer backbone was observed, consistent with unmodified polymer. Photoisomerization of the motor unit to the unstable (2′*S*)-(*P*)-*E*-**34** (estimated PSS *Z* : *E* – 21 : 79) isomer brings the naphthalene upper half of the motor in close proximity to the polymer chain and induces a preferred *M* helicity in the polyisocyanate. Subsequent thermal isomerization of the motor to form (2′*S*)-(*M*)-*E*-**34** at room temperature for 30 minutes fully reverses the motor helicity and brings the rotor part on the other side of the polymer chain, which translates to a helicity inversion of the polymer from *M* to *P* as indicated by the modulation of the CD absorptions. Continuing the rotational cycle by photoisomerization to the stable, the (2′*S*)-(*M*)-*Z*-**34** isomer moves the rotor away from the polymer chain end, which leads to reformation of the initial mixture of racemic polymers.

This example illustrates nicely how the helicity of the molecular motor can be transferred and amplified onto a macromolecular system. As the motor dopant can be continuously rotated in this example, one can imagine the whole system operating away from equilibrium. As long as light is provided as an energy source, the helix inversion of the polymer backbone should take place continuously as a consequence of the motors repeated helix inversion.

Looking at the step-by-step operation mode that was initially described for the modified polymer, the system appears to be limited by the thermal process. At room temperature, the THI takes 30 minutes to complete fully – faster or slower switching will require a temperature change that might have an effect on the properties of the

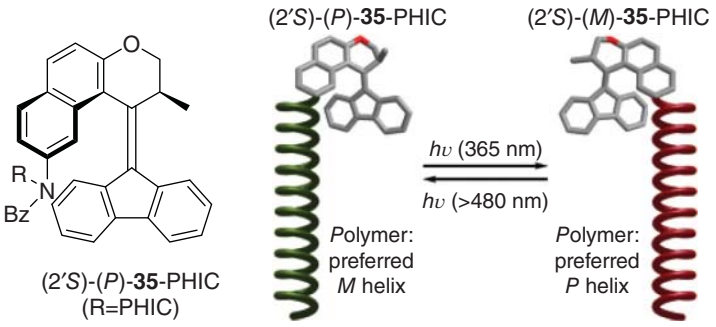

Figure 12.8 The bistable switch **35** attached to the chain end of a polyisocyanate can induce a fully light-controlled change in helicity of the polymer. When the switch adapts *P* helicity, the polymer chain has a preferential *M* helicity and vice versa. *Source:* From Pijper et al. [112]. © American Chemical Society.

liquid crystalline polymer itself. A system that is fully operated by light at a constant temperature allows a more precise control over the helicity of the liquid crystalline phase.

In 2008, our group reported a motor design that was adapted to these requirements (Figure 12.8) [112]. The motor was redesigned into a bistable chiroptical switch with two thermally stable isomers (at RT) instead of the four-step switching cycle in the parent design. The poly (*n*-hexyl isocyanate) (PHIC) polymer chain was attached to the upper half of the molecule in the fjord region of the switch, hampering the passage of the group along the lower part of the motor and therefore effectively blocking the THI step. The fluorenyl lower half was left unsubstituted, resulting in a symmetrical stator.

These structural modifications reduce the number of possible isomers to two thermally stable structures, the *P* and the *M* helical isomer, which can be interconverted in a fully reversible manner using light of two different wavelengths. (2′*S*)-(*P*)-**35**-PHIC induces an *M* helicity in the polyisocyanate backbone, and (2′*S*)-(*M*)-**35**-PHIC a *P* helicity. Not only is the occurrence of a racemic mixture within the switching cycle eliminated, but the induction of the preferred handedness is much more effective than in the previous design. This improvement is due to the fact that the polymer chain is positioned closer to the molecular motor than it was before, leading to a more pronounced induction of chirality.

Integration of the polymer–motor hybrid molecules in a LC matrix with subsequent irradiation experiments revealed that the sign and magnitude of the supramolecular helical pitch of the LC phase are fully controllable by light, in a completely reversible process.

Although the covalent attachment of molecular motors to polymer chains has been a successful strategy in controlling the properties of the obtained system by light, a noncovalent approach can offer alternative. The synthetic effort to create such a system would be reduced, and a more modular system could potentially arise from it. Hence, inspired by the work of Yashima and coworkers [124], our group sought to use a noncovalently attached molecular motor as chiral dopant to initiate

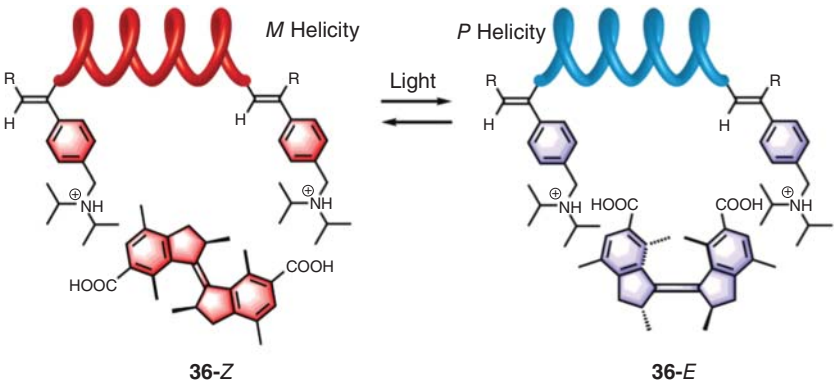

Figure 12.9 The helicity of polyisocyanate can be controlled by addition of a noncovalently attached carboxylate motor **36** as dopant. The *Z* isomer of the first-generation motor induces *P* helicity, while the *E* isomer induces *M* helicity. *Source:* van Leeuwen et al. [125]. © Royal Society of Chemistry.

an induction of helicity in a helical polymer [125]. A first-generation molecular motor used was therefore equipped with carboxylate side groups to interact with ammonium side groups of a polyphenylacetylene polymer via ionic interaction (Figure 12.9).

Of the four isomers in the rotational cycle of motor **36**, only three are accessible at room temperature since the THI from (*M*, *M*)-(*E*) to (*P*, *P*)-(*E*) is very fast. The stable (*P*, *P*)-(*Z*) isomer of motor **36** induces *M* helicity in the polymer chain. Switching to (*P*, *P*)-(*E*) through photoisomerization with immediate subsequent THI results in an induction of *P* helicity in the polymer chain, despite the fact that the motor has the same intrinsic *P* helicity in both *Z* and *E* isomers. Considering the differences between both isomers, the authors propose that the distance between the carboxyl groups is what induces the difference in preferred polymer helicity. They additionally indicate that the motor is likely to detach for the photoisomerization and reattach to switch the helicity of the polymer chain.

These results show that chirality of a molecular motor may also be transferred to a polymer chain via noncovalent interactions. The helix inversion could be performed in situ by light irradiation of a mixture of the dopant with the polymer chain.

12.8 Self-assembled Systems

Self-assembly is defined as the formation of a large ordered structure through noncovalent interactions of molecular building blocks [126, 127]. Small molecules assembling to form intricate structures of different shapes and sizes, like the formation of cell membranes from lipids, play a crucial role in living organisms.

For the scientist, self-assembly opens up the possibility to work with very complex systems and enhance functions through cooperativity without the need of complicated synthesis of elaborate single molecules. Just as in the living cell, the artificial self-assembly performed in the laboratory is a dynamic, error-correcting and reversible process. Tuning the noncovalent interactions between the different

building blocks in an assembly to obtain dynamic systems, while maintaining stability, plays a crucial role in this field of research. Several research groups have been focusing on responsive self-assembled materials that can be controlled by an external stimulus, such as light [9, 10, 126–128].

The first example of a self-assembled system based on molecular motors involved the study of amphiphilic structures in water [129]. This system represents the first demonstration of a motor that retained its function in aqueous environment, which is a major achievement on the way to using molecular motors in biomedical applications.

Amphiphilic structures consist of a hydrophobic moiety (like a long alkyl chain) and a hydrophilic moiety (like an ethylene glycol chain). Depending on the balance between both of these features, these molecules can assemble in a large variety of structures in water like micelles, vesicles, or fibers [130]. Additional interactions like π–π stacking or hydrogen bonding between the surfactants can generate more complex structures. The critical packing parameter, which is a combination of the length and volume of the hydrophobic moiety and the surface area of the hydrophilic moiety, can aid to a certain extent to predict the resulting assembled morphology from the structure of the amphiphile.

Based on a previously reported self-assembled nanotube, which could be disassembled upon light irradiation in an irreversible process [131], two new structures were designed in our group: a motor with an upper half featuring a five-membered ring and a relatively short half-life and one with an upper half with a six-membered ring, resulting in a long half-life [129]. To create the necessary amphiphilic properties, dodecyl chains were attached to the lower half and amine-terminated ethylene glycol chains to the upper half of both designs. The lower half was the same for both compounds and was designed to be symmetric. Therefore, there is no structural difference between the *E* and *Z* isomers. Both molecules form tubular structures in coassembly with dioleoyl-*sn*-glycero-3-phosphocholine (DOPC) (1 : 1) in water (Figure 12.10).

The slow motor completely adapts its morphology from the tubular structure toward a vesicular structure upon irradiation with light. The authors propose that the morphology change is not due to the movement of the molecular motor, but due to the difference in packing parameter between the stable isomer and the light-generated unstable isomer. Upon heating the aggregates, the molecular motor undergoes THI to the stable form, which takes place without any change in aggregate morphology. However, if given the chance to reassemble after freeze thawing the sample, the motor amphiphiles once again adopt a tubular structure. This process can be repeated multiple times.

In contrast, upon irradiation with light, the motor with a five-membered ring in the upper half showed neither a change in absorption spectra nor a change in morphology. This observation can be explained by considering that the half-life of the unstable state (4 ns at room temperature), as confirmed by transient absorption measurements, was simply too short to allow for the unstable form to be observed 12.10.

The tendency of motors to self-assemble in aqueous media was later exploited to study their rotational behavior in the confined space of nanospheres formed through solvent mixing (Figure 12.11) [132]. A highly lipophilic first-generation molecular

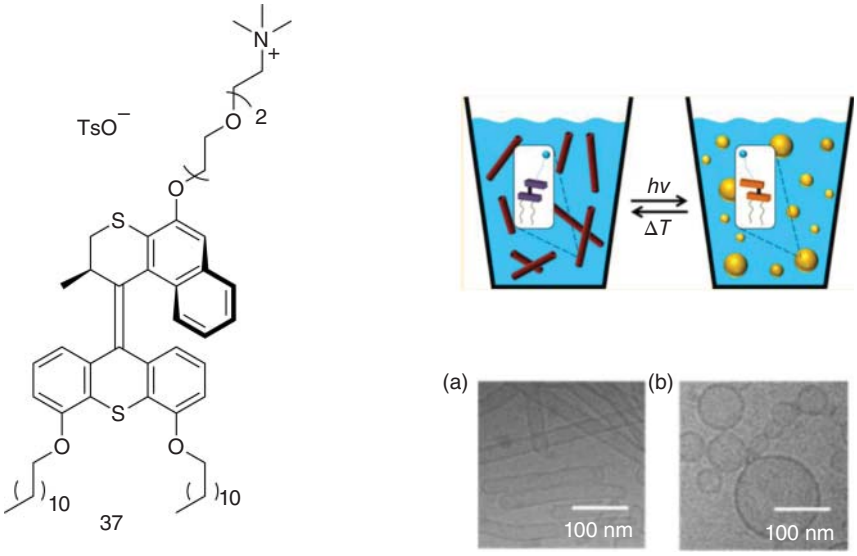

Figure 12.10 The stable and unstable isomers of photoswitch **37** form different shaped aggregates together with DOPC in aqueous solution (1 : 1 ratio). Both the nanotubes (stable **37**) and spherical aggregates (unstable **37**) can be interconverted reversibly, as demonstrated by cryo-TEM (bottom right). *Source:* From van Dijken et al. [129].

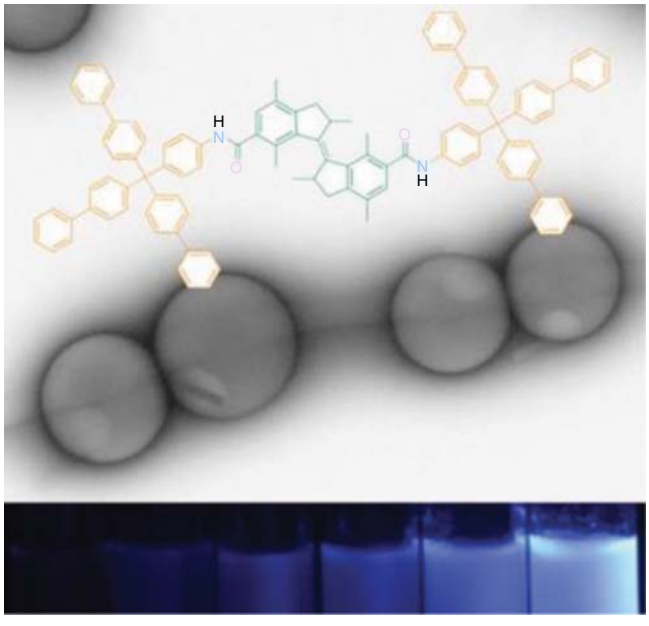

Figure 12.11 Bowl-shaped aggregates of different sizes can be formed in a solvent-assisted assembly. The rotation speed of the motor **38** can be influenced by the size of the confined space of the aggregate. *Source:* Reproduced with permission from Ref. Franken et al. [132]. Copyright 2008, American Chemical Society.

motor 38 equipped with bulky aromatic substituents on both halves of the molecule forms bowl-shaped particles by dissolution in an organic solvent and subsequent mixing with water. The size of the particles can be controlled by applying different solvent ratios and can even be increased or decreased by adding one or the other solvent after the particles are already formed. With an increasing amount of water in the mixture, the particle size decreases and with it the space provided for the motor to rotate. In a solution with a water content of 60%, the motor rotation is unhampered. Addition of 90% of water to the mixture has a large influence on the motors rotation through the decrease of the nanosphere size and increasing steric hindrance. The THI of unstable *Z* to form stable *Z* is blocked by the confined space; instead, a thermal back isomerization and formation of stable *E* occurs upon heating. Therefore, the level of confinement in water can be used to control the forward or backward isomerization of the motor.

On the quest to design an artificial muscle-type function, a more elaborate self-assembled system was presented in 2017 (Figure 12.12) [133, 134]. Biscarboxylate-based amphiphilic motors **39** were assembled via shear flow and calcium ion binding in a hierarchical organization in bundle-forming nanofibers. The formed strings were put under light irradiation in an aqueous solution. Within 60 seconds the string was bending in an angle of up to 90° toward the light source, showcasing not only a fast but also a large amplitude actuation through multiple length scales of the molecular movement to the movement of the whole assembled system, effectively harnessing the collective molecular motion. This actuating motion is particularly impressive when considering that the string consists of 95% water. The so-called molecular muscle was afterward subjected to weight-lifting experiments upon light irradiation of the strings in air, presenting its capability to lift pieces of paper of up to 0.4 mg in an angle of 50° (equals 0.05 μJ of mechanical work performed by the string).

It was proposed that the formation of the unstable isomer from the stable isomer upon light irradiation disturbs the packing arrangement locally on the one side of the string that is being irradiated. This leads to an expansion of the string diameter, as confirmed by Small Angle X-ray Scattering (SAXS), while the total volume of the string remains unchanged, resulting in a contraction of the long axis of the string,

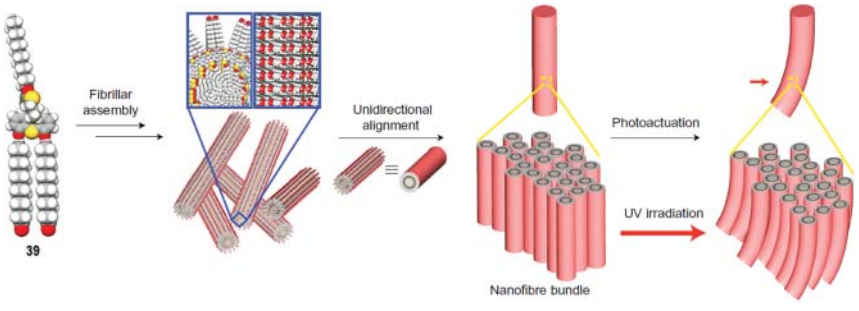

Figure 12.12 The amphiphilic motor **39** aggregates in fibers, which form bundles in a hierarchical assembly. Upon irradiation with UV light, the bundles bend toward the light source. *Source:* From Chen et al. [133]. © 2018, Springer Nature.

forcing it to bend. In this system, effective amplification of motion of small molecules in a supramolecular assembly along multiple length scales in water was achieved. The speed and amplitude of motion is critically dependent on the cations used to form the hierarchical organization [134].

This concept was extended, when the motor amphiphiles were functionalized with a histidine moiety and used as a template for the growth of magnetic iron oxide nanoparticles, allowing magnetic control of the resulting fibrous material additional to the light control. The system was subjected to cargo-transporting experiments, in which the fiber was used to pick up small pieces of paper upon light irradiation, guided to a different position by a magnet and subsequently releasing the cargo again assisted by light [135].

While the functioning of these self-assembled muscles is ultimately based on switching rather than unidirectional rotation, the large amplitude effects observed constitute an impressive showcase for the potential of molecular motors to amplify and traverse length scales. Ratcheting of the actuation process may lead to these soft actuators performing real net work.

12.9 Conclusion

With overcrowded alkene-based molecular motors, we already have the world's smallest out-of-equilibrium system in hand. They are a fascinating class of compounds that perform continuous rotational movement in only one direction as long as energy is supplied to the system. Once the influx of energy ceases, the system relaxes thermally and adopts an equilibrium state. In addition to these light-driven systems, opportunities and challenges lie in the development of genuine catalytic [23, 24] and electrical (redox) driven rotary motors [136].

Moving forward in molecular motors research, the question therefore is no longer how to develop an out-of-equilibrium system, but how to use the inherent capability of the molecule to dissipate energy and operate away from thermal equilibrium to perform useful functions and generate work, ranging from the nano- to the macroscale.

Several strategies for the creation of motorized supramolecular systems have been pursued over the last two decades, including surface anchoring, self-assemblies of amphiphiles, or the immobilization of the molecules in 3D materials, like polymers and MOFs. All the systems synthesized can be operated by light in a noninvasive manner, inducing dynamic and often reversible changes of the material structure. Most of the systems described in this chapter ultimately rely on the functioning of molecular motors as bistable switches. The results have often been impressive, and by now it should be evident that small amounts of motor can generate tremendous effects and can perform tasks such as moving and lifting macroscopic objects.

However, creating systems in which the out-of-equilibrium properties of the molecular motor are amplified and their full potential is exploited in practical use still remains a major challenge. A number of systems presented in this chapter, most notably Feringa's nanocar [72], Giuseppone's polymer [95], and Katsonis'

chiral LC structures [122] serve as examples of the tremendous opportunities of these compounds to perform work away from the thermodynamic equilibrium.

Amplifying and utilizing the unidirectional rotation of a molecular motor is arguably the most important challenge currently ahead of us. Future efforts will also focus on the integration of molecular motors in materials and their rotation in unison, in order to achieve macroscopic effects. It is not only the immobilization of the molecules that is important to achieve collaborative movement but also the relative positional and orientational alignment of multiple motors. The organization of motors in metal organic frameworks and in hierarchical self-assembled materials serve as great examples for such applications. To generate collective effects with a net output, the integration of enantiomerically pure material will be necessary.

Regarding the current state of the art, it is clear that molecular motors research is entering a new era. Combining the out-of-equilibrium properties of a molecular motor, years of experience in constructing systems capable of collective output, and novel synthetic methods that allow us to synthesize large quantities of (optically pure) material, we possess all the tools required to build smart systems capable of a net output of work. The coming decade will reveal whether molecular motors are able to make an impact at the macroscale of the same magnitude they already have at the nanoscale.

References

1 Binnig, G., Rohrer, H., Gerber, C., and Weibel, E. (1982). Surface studies by scanning tunneling microscopy. *Phys. Rev. Lett.* 49 (1): 57–61.

2 Berman, H., Henrick, K., and Nakamura, H. (2003). Announcing the worldwide protein data bank. *Nat. Struct. Biol.* 10 (12): 980.

3 Jhoti, H. and Leach, A.R. (2007). *Structure-based Drug Discovery*. Amsterdam, Netherlands: Springer Netherlands.

4 Ghosh, S.K. (2009). *Self-healing Materials: Fundamentals, Design Strategies, and Applications*. Weinheim, Germany: Wiley-VCH.

5 Whitesides, G.M. (2018). Soft robotics. *Angew. Chem. Int. Ed.* 57 (16): 4258–4273.

6 Liu, D., Yang, F., Xiong, F., and Gu, N. (2016). The smart drug delivery system and its clinical potential. *Theranostics* 6 (9): 1306–1323.

7 Lancia, F., Ryabchun, A., and Katsonis, N. (2019). Life-like motion driven by artificial molecular machines. *Nat. Rev. Chem.* 3 (9): 536–551.

8 Browne, W.R. and Feringa, B.L. (2006). Making molecular machines work. *Nat. Nanotechnol.* 1 (1): 25–35.

9 Mattia, E. and Otto, S. (2015). Supramolecular systems chemistry. *Nat. Nanotechnol.* 10 (2): 111–119.

10 Kathan, M. and Hecht, S. (2017). Photoswitchable molecules as key ingredients to drive systems away from the global thermodynamic minimum. *Chem. Soc. Rev.* 46 (18): 5536–5550.

11 Goodsell, D.S. (1992). *The Machinery of Life*. New York, NY: Copernicus Books.

12 Balzani, V., Credi, A., Raymo, F., and Stoddart, J.F. (2000). *Artificial molecular machines*. *Angew. Chem. Int. Ed.* 39 (19): 3348–3391.

13 Balzani, V., Credi, A., and Venturi, M. (2009). Light powered molecular machines. *Chem. Soc. Rev.* 38 (6): 1542–1550.

14 Erbas-Cakmak, S., Leigh, D.A., McTernan, C.T., and Nussbaumer, A.L. (2015). Artificial molecular machines. *Chem. Rev.* 115 (18): 10081–10206.

15 Kassem, S., Van Leeuwen, T., Lubbe, A.S. et al. (2017). Artificial molecular motors. *Chem. Soc. Rev.* 46 (9): 2592–2621.

16 Sauvage, J.-P. and Gaspard, P. (eds.) (2010). *From Non-Covalent Assemblies to Molecular Machines*. Weinheim, Germany: Wiley-VCH.

17 Kinbara, K. and Aida, T. (2005). Toward intelligent molecular machines: directed motions of biological and artificial molecules and assemblies. *Chem. Rev.* 105 (4): 1377–1400.

18 Muller, P. (1994). Glossary of terms used in physical organic chemistry (IUPAC Recommendations 1994). *Pure Appl. Chem.* 66 (5): 1077–1184.

19 Astumian, R.D. (2007). Design principles for Brownian molecular machines: how to swim in molasses and walk in a hurricane. *Phys. Chem. Chem. Phys.* 9 (37): 5067–5083.

20 Astumian, R.D. (2012). Microscopic reversibility as the organizing principle of molecular machines. *Nat. Nanotechnol.* 7 (11): 684–688.

21 Feringa, B.L., Jager, W.F., de Lange, B., and Meijer, E.W. (1991). Chiroptical molecular switch. *J. Am. Chem. Soc.* 113 (14): 5468–5470.

22 Kelly, T.R., De Silva, H., and Silva, R.A. (1999). Unidirectional rotary motion in a molecular system. *Nature* 401 (6749): 150–152.

23 Fletcher, S.P., Dumur, F., Pollard, M.M., and Feringa, B.L. (2005). A reversible, unidirectional molecular rotary motor driven by chemical energy. *Science* 310 (5745): 80–82.

24 Collins, B.S.L., Kistemaker, J.C.M., Otten, E., and Feringa, B.L. (2016). A chemically powered unidirectional rotary molecular motor based on a palladium redox cycle. *Nat. Chem.* 8 (9): 860–866.

25 Erbas-Cakmak, S., Fielden, S.D.P., Karaca, U. et al. (2017). Rotary and linear molecular motors driven by pulses of a chemical fuel. *Science* 358 (6361): 340–343.

26 Koumura, N., Zijlstra, R.W., van Delden, R.A. et al. (1999). Light-driven monodirectional molecular rotor. *Nature* 401 (6749): 152–155.

27 ter Wiel, M.K.J., van Delden, R.A., Meetsma, A., and Feringa, B.L. (2005). Light-driven molecular motors: stepwise thermal helix inversion during unidirectional rotation of sterically overcrowded biphenanthrylidenes. *J. Am. Chem. Soc.* 127 (41): 14208–14222.

28 Koumura, N., Geertsema, E.M., Meetsma, A., and Feringa, B.L. (2000). Light-driven molecular rotor: unidirectional rotation controlled by a single stereogenic center. *J. Am. Chem. Soc.* 122 (48): 12005–12006.

29 Kistemaker, J.C.M., Pizzolato, S.F., van Leeuwen, T. et al. (2016). Spectroscopic and theoretical identification of two thermal isomerization pathways for bistable chiral overcrowded alkenes. *Chem. Eur. J.* 22 (38): 13478–13487.

30 Koumura, N., Geertsema, E.M., van Gelder, M.B. et al. (2002). Second generation light-driven molecular motors. Unidirectional rotation controlled by a single stereogenic center with near-perfect photoequilibria and acceleration of the speed of rotation by structural modification. *J. Am. Chem. Soc.* 124 (18): 5037–5051.

31 Kistemaker, J.C.M., Štacko, P., Visser, J., and Feringa, B.L. (2015). Unidirectional rotary motion in achiral molecular motors. *Nat. Chem.* 7 (11): 890–896.

32 Chen, K.-Y. (2014). Multivalent molecular motors for surface attachment. PhD thesis, University of Groningen, Netherlands.

33 Klok, M. (2009). Motors for use in molecular nanotechnology. PhD thesis, University of Groningen, Netherlands.

34 Vicario, J., Meetsma, A., and Feringa, B.L. (2005). Controlling the speed of rotation in molecular motors. Dramatic acceleration of the rotary motion by structural modification. *Chem. Commun.*: 5910–5912.

35 Koumura, N., ter Wiel, M.K.J., Meetsma, A. et al. (2002). In control of the speed of rotation in molecular motors. Unexpected retardation of rotary motion. *Chem. Commun.*: 2962–2963.

36 Pollard, M.M., Wesenhagen, P.V., Pijper, D., and Feringa, B.L. (2008). On the effect of donor and acceptor substituents on the behaviour of light-driven rotary molecular motors. *Org. Biomol. Chem.* 6 (9): 1605–1612.

37 Vicario, J., Walko, M., Meetsma, A., and Feringa, B.L. (2006). Fine tuning of the rotary motion by structural modification in light-driven unidirectional molecular motors. *J. Am. Chem. Soc.* 128 (15): 5127–5135.

38 Bauer, J., Hou, L., Kistemaker, J.C.M., and Feringa, B.L. (2014). Tuning the rotation rate of light-driven molecular motors. *J. Org. Chem.* 79 (10): 4446–4455.

39 Klok, M., Boyle, N., Pryce, M.T. et al. (2008). MHz unidirectional rotation of molecular rotary motors. *J. Am. Chem. Soc.* 130 (32): 10484–10485.

40 Kistemaker, J.C.M. (2017). Autonomy and chirality in molecular motors. PhD thesis, University of Groningen, Netherlands.

41 Faulkner, A., van Leeuwen, T., Feringa, B.L., and Wezenberg, S.J. (2016). Allosteric regulation of the rotational speed in a light-driven molecular motor. *J. Am. Chem. Soc.* 138 (41): 13597–13603.

42 Dorel, R., Miró, C., Wei, Y. et al. (2018). Cation-modulated rotary speed in a light-driven crown ether functionalized molecular motor. *Org. Lett.* 20 (13): 3715–3718.

43 van Leeuwen, T., Danowski, W., Pizzolato, S.F. et al. (2018). Braking of a light-driven molecular rotary motor by chemical stimuli. *Chem. Eur. J.* 24 (1): 81–84.

44 Qu, D.-H. and Feringa, B.L. (2010). Controlling molecular rotary motion with a self-complexing lock. *Angew. Chem. Int. Ed.* 49 (6): 1107–1110.

45 Roke, D., Stuckhardt, C., Danowski, W. et al. (2018). Light-gated rotation in a molecular motor functionalized with a dithienylethene switch. *Angew. Chem. Int. Ed.* 57 (33): 10515–10519.

46 Lerch, M.M., Hansen, M.J., van Dam, G.M. et al. (2016). Emerging targets in photopharmacology. *Angew. Chem. Int. Ed.* 55 (37): 10978–10999.

47 Wezenberg, S.J., Chen, K.-Y., and Feringa, B.L. (2015). Visible-light-driven photoisomerization and increased rotation speed of a molecular motor acting as a ligand in a ruthenium(II) complex. *Angew. Chem. Int. Ed.* 54 (39): 11457–11461.

48 Cnossen, A., Hou, L., Pollard, M.M. et al. (2012). Driving unidirectional molecular rotary motors with visible light by intra- and intermolecular energy transfer from palladium porphyrin. *J. Am. Chem. Soc.* 134 (42): 17613–17619.

49 van Leeuwen, T., Pol, J., Roke, D. et al. (2017). Visible-light excitation of a molecular motor with an extended aromatic core. *Org. Lett.* 19 (6): 1402–1405.

50 Roke, D., Feringa, B.L., and Wezenberg, S.J. (2019). A visible-light-driven molecular motor based on pyrene. *Helv. Chim. Acta* 102: e1800221.

51 van Delden, R.A., Koumura, N., Schoevaars, A. et al. (2003). A donor–acceptor substituted molecular motor: unidirectional rotation driven by visible light. *Org. Biomol. Chem.* 1: 33–35.

52 Pfeifer, L., Scherübl, M., Fellert, M. et al. (2019). Photoefficient 2nd generation molecular motors responsive to visible light. *Chem. Sci.* 10: 8768–8773.

53 Roke, D., Sen, M., Danowski, W. et al. (2019). Visible-light-driven tunable molecular motors based on oxindole. *J. Am. Chem. Soc.* 141 (18): 7622–7627.

54 Guentner, M., Schildhauer, M., Thumser, S. et al. (2015). Sunlight-powered kHz rotation of a hemithioindigo-based molecular motor. *Nat. Commun.* 6: 8406.

55 Ruangsupapichat, N., Pollard, M.M., Harutyunyan, S.R., and Feringa, B.L. (2011). Reversing the direction in a light-driven rotary molecular motor. *Nat. Chem.* 3 (1): 53–60.

56 Neubauer, T.M., van Leeuwen, T., Zhao, D. et al. (2014). Asymmetric synthesis of first generation molecular motors. *Org. Lett.* 16: 4220–4223.

57 van Leeuwen, T., Danowski, W., Otten, E. et al. (2017). Asymmetric synthesis of second-generation light-driven molecular motors. *J. Org. Chem.* 82 (10): 5027–5033.

58 Tietze, L.F., Düfert, A., Lotz, F. et al. (2009). Synthesis of chiroptical molecular switches by Pd-catalyzed domino reactions. *J. Am. Chem. Soc.* 131 (49): 17879–17884.

59 Pijper, T.C., Pijper, D., Pollard, M.M. et al. (2010). An enantioselective synthetic route toward second-generation light-driven rotary molecular motors. *J. Org. Chem.* 75 (3): 825–838.

60 van Leeuwen, T., Gan, J., Kistemaker, J.C.M. et al. (2016). Enantiopure functional molecular motors obtained by a switchable chiral-resolution process. *Chem. Eur. J.* 22 (21): 7054–7058.

61 Li, Q., Foy, J.T., Colard-Itté, J.R. et al. (2017). Gram scale synthesis of functionalized and optically pure Feringa's motors. *Tetrahedron* 73: 4874–4882.

62 Coskun, A., Banaszak, M., Astumian, R.D. et al. (2012). Great expectations: can artificial molecular machines deliver on their promise? *Chem. Soc. Rev.* 41 (1): 19–30.

63 Feringa, B.L. and Browne, W.R. (eds.) (2011). *Molecular Switches*. Weinheim, Germany: Wiley-VCH.

64 von Delius, M. and Leigh, D.A. (2011). Walking molecules. *Chem. Soc. Rev.* 40 (7): 3656–3676.

65 Pezzato, C., Cheng, C., Stoddart, J.F., and Astumian, R.D. (2017). Mastering the non-equilibrium assembly and operation of molecular machines. *Chem. Soc. Rev.* 46: 5491–5507.

66 Astumian, R.D. (2018). Trajectory and cycle-based thermodynamics and kinetics of molecular machines: the importance of microscopic reversibility. *Acc. Chem. Res.* 51: 2653–2661.

67 Abendroth, J.M., Bushuyev, O.S., Weiss, P.S., and Barrett, C.J. (2015). Controlling motion at the nanoscale: rise of the molecular machines. *ACS Nano* 9 (8): 7746–7768.

68 Sasaki, T. and Tour, J.M. (2007). Synthesis of a dipolar nanocar. *Tetrahedron Lett.* 48 (33): 5821–5824.

69 Sasaki, T., Osgood, A.J., Alemany, L.B. et al. (2008). Synthesis of a nanocar with an angled chassis. Toward circling movement. *Org. Lett.* 10 (2): 229–232.

70 Shirai, Y., Osgood, A.J., Zhao, Y. et al. (2005). Directional control in thermally driven single-molecule nanocars. *Nano Lett.* 5 (11): 2330–2334.

71 Morin, J.F., Shirai, Y., and Tour, J.M. (2006). En route to a motorized nanocar. *Org. Lett.* 8 (8): 1713–1716.

72 Kudernac, T., Ruangsupapichat, N., Parschau, M. et al. (2011). Electrically driven directional motion of a four-wheeled molecule on a metal surface. *Nature* 479 (7372): 208–211.

73 Saywell, A., Bakker, A., Mielke, J. et al. (2016). Light-induced translation of motorized molecules on a surface. *ACS Nano* 10 (12): 10945–10952.

74 García-López, V., Chen, F., Nilewski, L.G. et al. (2017). Molecular machines open cell membranes. *Nature* 548 (7669): 567–572.

75 Liu, D., Garcia-Lopez, V., Gunasekera, R.S. et al. (2019). Near-infrared light activates molecular nanomachines to drill into and kill cells. *ACS Nano* 13 (6): 6813–6823.

76 Lubbe, A.S., Kistemaker, J.C.M., Smits, E.J., and Feringa, B.L. (2016). Solvent effects on the thermal isomerization of a rotary molecular motor. *Phys. Chem. Chem. Phys.* 18: 26725–26735.

77 Kistemaker, J.C.M., Lubbe, A.S., Bloemsma, E.A., and Feringa, B.L. (2016). On the role of viscosity in the eyring equation. *ChemPhysChem* 17 (12): 1819–1822.

78 Chen, J., Kistemaker, J.C.M., Robertus, J., and Feringa, B.L. (2014). Molecular stirrers in action. *J. Am. Chem. Soc.* 136 (42): 14924–14932.

79 Caroli, G., Kwit, M.G., and Feringa, B.L. (2008). Photochemical and thermal behavior of light-driven unidirectional molecular motor with long alkyl chains. *Tetrahedron* 64: 5956–5962.

80 Doolittle, A.K. (1951). Studies in Newtonian flow II. The dependence of the viscosity of liquids on free-space. *J. Appl. Phys.* 22: 1471–1475.

81 García-López, V., Chiang, P.T., Chen, F. et al. (2015). Unimolecular submersible nanomachines. Synthesis, actuation, and monitoring. *Nano Lett.* 15 (12): 8229–8239.

82 Dorel, R. and Feringa, B.L. (2019). Photoswitchable catalysis based on the isomerisation of double bonds. *Chem. Commun.* 55: 6477–6486.

83 van Delden, R.A., ter Wiel, M.K.J., Pollard, M.M. et al. (2005). Unidirectional molecular motor on a gold surface. *Nature* 437 (7063): 1337–1340.

84 Pollard, M.M., Lubomska, M., Rudolf, P., and Feringa, B.L. (2007). Controlled rotary motion in a monolayer of molecular motors. *Angew. Chem. Int. Ed.* 46 (8): 1278–1280.

85 Carroll, G.T., Pollard, M.M., van Delden, R.A., and Feringa, B.L. (2010). Controlled rotary motion of light-driven molecular motors assembled on a gold film. *Chem. Sci.* 1 (1): 97–101.

86 Vachon, J., Carroll, G.T., Pollard, M.M. et al. (2014). An ultrafast surface-bound photo-active molecular motor. *Photochem. Photobiol. Sci.* 13 (2): 241–246.

87 Pollard, M.M., ter Wiel, M.K.J., van Delden, R.A. et al. (2008). Light-driven rotary molecular motors on gold nanoparticles. *Chem. Eur. J.* 14 (36): 11610–11622.

88 Chen, J., Chen, K.-Y., Carroll, G.T., and Feringa, B.L. (2014). Facile assembly of light-driven molecular motors onto a solid surface. *Chem. Commun.* 50: 12641–12644.

89 London, G., Carroll, G.T., Fernández Landaluce, T. et al. (2009). Light-driven altitudinal molecular motors on surfaces. *Chem. Commun.*: 1712–1714.

90 London, G., Chen, K.-Y., Carroll, G.T., and Feringa, B.L. (2013). Towards dynamic control of wettability by using functionalized altitudinal molecular motors on solid surfaces. *Chem. Eur. J.* 19 (32): 10690–10697.

91 Chen, K.-Y., Wezenberg, S.J., Carroll, G.T. et al. (2014). Tetrapodal molecular switches and motors: synthesis and photochemistry. *J. Org. Chem.* 79 (15): 7032–7040.

92 Chen, K.-Y., Ivashenko, O., Carroll, G.T. et al. (2014). Control of surface wettability using tripodal light-activated molecular motors. *J. Am. Chem. Soc.* 136 (8): 3219–3224.

93 Carroll, G.T., London, G., Landaluce, T.F. et al. (2011). Adhesion of photon-driven molecular motors to surfaces via 1,3-dipolar cycloadditions: effect of interfacial interactions on molecular motion. *ACS Nano* 5 (1): 622–630.

94 Kaleta, J., Chen, J., Bastien, G. et al. (2017). Surface inclusion of unidirectional molecular motors in hexagonal tris(*o*-phenylene)cyclotriphosphazene. *J. Am. Chem. Soc.* 139 (30): 10486–10498.

95 Li, Q., Fuks, G., Moulin, E. et al. (2015). Macroscopic contraction of a gel induced by the integrated motion of light-driven molecular motors. *Nat. Nanotechnol.* 10 (2): 161–165.

96 Foy, J.T., Li, Q., Goujon, A. et al. (2017). Dual-light control of nanomachines that integrate motor and modulator subunits. *Nat. Nanotechnol.* 12 (6): 540–545.

97 Danowski, W., van Leeuwen, T., Abdolahzadeh, S. et al. (2019). Unidirectional rotary motion in a metal–organic framework. *Nat. Nanotechnol.* 14 (5): 488–494.

98 Yaghi, O.M., Kalmutzki, M.J., and Diercks, C.S. (eds.) (2019). *Introduction to Reticular Chemistry*. Weinheim, Germany: Wiley-VCH.

99 Rowsell, J.L.C. and Yaghi, O.M. (2004). Metal-organic frameworks: a new class of porous materials. *Microporous Mesoporous Mater.* 73 (1–2): 3–14.

100 Deng, H., Olson, M.A., Stoddart, J.F., and Yaghi, O.M. (2010). Robust dynamics. *Nat. Chem.* 2 (6): 439–443.

101 Yaghi, O.M., O'Keeffe, M., Ockwig, N.W. et al. (2003). Reticular synthesis and the design of new materials. *Nature* 423 (6941): 705–714.

102 Martinez-Bulit, P., Stirk, A.J., and Loeb, S.J. (2019). Rotors, motors, and machines inside metal-organic frameworks. *Trends Chem.* 1 (6): 588–600.

103 Gonzalez-Nelson, A., Coudert, F.X., and van der Veen, M.A. (2019). Rotational dynamics of linkers in metal–organic frameworks. *Nanomaterials* 9 (3): 330.

104 Karagiaridi, O., Bury, W., Mondloch, J.E. et al. (2014). Solvent-assisted linker exchange: an alternative to the de novo synthesis of unattainable metal-organic frameworks. *Angew. Chem. Int. Ed.* 53 (18): 4530–4540.

105 Blackmond, D.G. (2010). The origin of biological homochirality. *Cold Spring Harb. Perspect. Biol.* 2 (5): a002147–a002147.

106 Feringa, B.L. and Delden, R.A. (1999). Absolute asymmetric synthesis: the origin, control, and amplification of chirality. *Angew. Chem. Int. Ed.* 38 (23): 3418–3438.

107 van Delden, R.A. and Feringa, B.L. (2001). Color indicators of molecular chirality based on doped liquid crystals. *Angew. Chem. Int. Ed.* 40 (17): 3198–3200.

108 Yashima, E., Maeda, K., and Nishimura, T. (2004). Detection and amplification of chirality by helical polymers. *Chem. Eur. J.* 10 (1): 42–51.

109 Wilson, A.J., Masuda, M., Sijbesma, R.P., and Meijer, E.W. (2005). Chiral amplification in the transcription of supramolecular helicity into a polymer backbone. *Angew. Chem. Int. Ed.* 44 (15): 2275–2279.

110 Hirschberg, J.H.K.K., Brunsveid, L., Ramzi, A. et al. (2000). Helical self-assembled polymers from cooperative stacking of hydrogen-bonded pairs. *Nature* 407 (6801): 167–170.

111 Engelkamp, H., Middelbeek, S., and Nolte, R.J.M. (1999). Self-assembly of disk-shaped molecules to coiled-coil aggregates with tunable helicity. *Science* 284 (5415): 785–788.

112 Pijper, D., Jongejan, M.G.M., Meetsma, A., and Feringa, B.L. (2008). Light-controlled supramolecular helicity of a liquid crystalline phase using a helical polymer functionalized with a single chiroptical molecular switch. *J. Am. Chem. Soc.* 130 (13): 4541–4552.

113 Pijper, D. and Feringa, B.L. (2007). Molecular transmission: controlling the twist sense of a helical polymer with a single light-driven molecular motor. *Angew. Chem. Int. Ed.* 46 (20): 3693–3696.

114 Eelkema, R., Pollard, M.M., Vicario, J. et al. (2006). Molecular machines: nanomotor rotates microscale objects. *Nature* 440 (7081): 163.

115 Eelkema, R. and Feringa, B.L. (2006). Amplification of chirality in liquid crystals. *Org. Biomol. Chem.* 4 (20): 3729–3745.

116 Eelkema, R. and Feringa, B.L. (2006). Reversible full-range color control of a cholesteric liquid-crystalline film by using a molecular motor. *Chem. Asian J.* 1 (3): 367–369.

117 Feringa, B.L., Huck, N.P.M., and van Doren, H.A. (1995). Chiroptical switching between liquid crystalline phases. *J. Am. Chem. Soc.* 117 (39): 9929–9930.

118 van Delden, R.A., van Gelder, M.B., Huck, N.P.M., and Feringa, B.L. (2003). Controlling the color of cholesteric liquid-crystalline films by photoirradiation of a chiroptical molecular switch used as dopant. *Adv. Funct. Mater.* 13 (4): 319–324.

119 van Delden, R.A., Koumura, N., Harada, N., and Feringa, B.L. (2002). Unidirectional rotary motion in a liquid crystalline environment: color tuning by a molecular motor. *Proc. Natl. Acad. Sci. U. S. A.* 99 (8): 4945–4949.

120 Eelkema, R., Pollard, M.M., Katsonis, N. et al. (2006). Rotational reorganization of doped cholesteric liquid crystalline films. *J. Am. Chem. Soc.* 128 (44): 14397–14407.

121 Chen, J., Lacaze, E., Brasselet, E. et al. (2014). Textures of cholesteric droplets controlled by photo-switching chirality at the molecular level. *J. Mater. Chem. C* 2 (38): 8137–8141.

122 Orlova, T., Lancia, F., Loussert, C. et al. (2018). Revolving supramolecular chiral structures powered by light in nanomotor-doped liquid crystals. *Nat. Nanotechnol.* 13 (4): 304–308.

123 Green, M.M., Andreola, C., Muñoz, B., and Reidy, M.P. (1988). Macromolecular stereochemistry: a cooperative deuterium isotope effect leading to a large optical rotation. *J. Am. Chem. Soc.* 110: 4063–4065.

124 Onouchi, H., Miyagawa, T., Morino, K., and Yashima, E. (2006). Assisted formation of chiral porphyrin homoaggregates by an induced helical poly(phenylacetylene) template and their chiral memory. *Angew. Chem. Int. Ed.* 45 (15): 2381–2384.

125 van Leeuwen, T., Heideman, G.H., Zhao, D. et al. (2017). In situ control of polymer helicity with a non-covalently bound photoresponsive molecular motor dopant. *Chem. Commun.* 53 (48): 6393–6396.

126 van Rossum, S.A.P., Tena-Solsona, M., van Esch, J.H. et al. (2017). Dissipative out-of-equilibrium assembly of man-made supramolecular materials. *Chem. Soc. Rev.* 46 (18): 5519–5535.

127 Grzybowski, B.A., Wilmer, C.E., Kim, J. et al. (2009). Self-assembly: from crystals to cells. *Soft Matter* 5: 1110–1128.

128 van Esch, J.H., Klajn, R., and Otto, S. (2017). Chemical systems out of equilibrium. *Chem. Soc. Rev.* 46: 5474–5475.

129 van Dijken, D.J., Chen, J., Stuart, M.C.A. et al. (2016). Amphiphilic molecular motors for responsive aggregation in water. *J. Am. Chem. Soc.* 138 (2): 660–669.

130 Israelachvili, J. (2011). *Intermolecular and Surface Forces*. Elsevier.

131 Coleman, A.C., Beierle, J.M., Stuart, M.C.A. et al. (2011). Light-induced disassembly of self-assembled vesicle-capped nanotubes observed in real time. *Nat. Nanotechnol.* 6 (9): 547–552.

132 Franken, L.E., Wei, Y., Chen, J. et al. (2018). Solvent mixing to induce molecular motor aggregation into bowl-shaped particles: underlying mechanism, particle nature, and application to control motor behavior. *J. Am. Chem. Soc.* 140 (25): 7860–7868.

133 Chen, J., Leung, F.K.-C., Stuart, M.C.A. et al. (2018). Artificial muscle-like function from hierarchical supramolecular assembly of photoresponsive molecular motors. *Nat. Chem.* 10 (2): 132–138.

134 Leung, F.K.-C., van den Enk, T., Kajitani, T. et al. (2018). Supramolecular packing and macroscopic alignment controls actuation speed in macroscopic strings of molecular motor amphiphiles. *J. Am. Chem. Soc.* 140: 17724–17733.

135 Leung, F.K.-C., Kajitani, T., Stuart, M.C.A. et al. (2019). Dual-controlled macroscopic motions in a supramolecular hierarchical assembly of motor amphiphiles. *Angew. Chem. Int. Ed.* 58 (32): 10985–10989.

136 Logtenberg, H., Areephong, J., Bauer, J. et al. (2016). Towards redox-driven unidirectional molecular motion. *ChemPhysChem* 17: 1895–1901.